UNIVERSITÀ DEGLI STUDI DEL MOLISE
Dipartimento di Bioscienze e Territorio

Dottorato di ricerca in
SCIENZE E TECNOLOGIE BIOLOGICHE ED AMBIENTALI

XXVI Ciclo

TESI

S.S.D. AGR/05

"DETECTION OF THE EFFECTS OF WATER STRESS ON WOODY PLANTS"

Tutor
Prof. Roberto Tognetti

Dottorando
Giovanni Marino

Coordinatore
Prof. Claudio Caprari

Supervisore CNR
Dott. Mauro Centritto

Anno Accademico 2013 / 2014

Table of Contents

CHAPTER 1 – Introduction

Water deficits occur in plants when the demand of evapotranspiration exceeds the supply of water in the soil (Slatyer, 1967). Soil water deficit is considered to be the main environmental factor limiting global plant photosynthesis (Nemani et al., 2003). In a global warming scenario that projects the effects of increasing atmospheric concentration of greenhouse gasses, climate models predict an increase of drought in the 21st century over many world regions, including Mediterranean basin (Dai, 2011), enhancing the incidence of water deficit stress on natural vegetation and crops (Rosenzweig et al., 2001). The effects of the combination of drought and warmer conditions on vegetation can be severe, as highlighted by regional-scale woody-plant die-off monitoring (Muller et al., 2005; Breshears et al., 2005; Allen et al., 2007). Drought stress reduces plant growth and crop yield, limits leaf area development, stem extension and root proliferation (Farooq et al., 2009). The reduction in turgor pressure, consequent to soil water deficit, affects sensitively the physiological processes involved in plant cell growth (Taiz & Zeiger, 2006).

Water stress induces stomatal closure, which reduces the transpiration rate, decreasing evaporative cooling and increasing leaf temperature. Furthermore, the inhibition of transpirational flow of sap, consequent to stomatal closure, can affect the absorption and transport of inorganic nutrients from roots to shoots (Garg, 2003). Nevertheless, photosynthesis reduction is one of major effects of drought and is aroused by stomatal limitations that reduce the CO_2 uptake, but even by non-stomatal limitations that compromise substantially the photosynthetic efficiency (Farooq et al., 2009). In fact, drought stress produced changes in photosynthetic apparatus, in the composition of photosynthetic pigments and reduces the activities of Calvin cycle enzymes (Flexas & Medrano, 2002). Stomatal closure responds more to soil moisture content than to leaf water status, suggesting the existence of a feedback response involving chemical signals from dehydrating roots (Davies & Zhang, 1991).

Water stress also stimulates the photorespiratory pathway, leading to the production of reactive oxygen species causing oxidative damage and affecting the normal functions of cells (Blokhina et al., 2003) and soliciting the production of antioxidant enzymes.

A reactive oxygen quenching mechanism and an antioxidant function have been supposed also for isoprene, meanly during simultaneous light and heat stress (Peñuelas et al., 2005). Isoprene is the most abundant phytogenic organic volatile compound (VOC) emitted by many forest species and is produced enzymatically, released from photosynthetically active tissues in the light and emitted through stomata to the atmosphere (Sharkey & Yeh, 2001). Isoprene biosynthesis is light dependent and is closely linked with carbon metabolism at ambient CO_2 concentration (Monson & Fall, 1989;

Loreto & Sharkey, 1990). Though, when photosynthesis is constrained by water stress, the biosynthesis and the emission of isoprene from leaves seems to be not affected and, in some cases, even enhanced by moderate stress (Beckett et al., 2012), suggesting that the synthesis of isoprene allows to avoid an excess of reducing power determined by a strong electron transport rate and a low photosynthetic capacity.

Analyzing and monitoring all the aforementioned responses of plants under water stress condition allows to understand the mechanisms of adaptation and defense adopted by plants to an environment that prospect to be more arid. The present PhD thesis gathers three different eco-physiological studies performed on agroforestry woody species with the aim of propose large scale techniques to the detection and the monitoring of plant water status and improve the knowledge of the parameters indicative of water stress and the mechanisms that correlate each other the different physiological responses of plants to water deficit.

References

Allen, C.D, Breshears, D.D., 2007. Climate-induced forest dieback as an emergent global phenomenon. Eos. Trans. Am. Geophys. Union. 88:504.

Blokhina O., Virolainen E., Fagerstedt K.V. (2003) Antioxidants, oxidative damage and oxygen deprivation stress: a review, Ann. Bot. 91, 179–194.

Breshears, et al. 2005, Regional vegetation die-off in response to global-change-type drought. Proc. Natl. Acad. Sci. USA 102:15144–15148.

Dai, A., 2011. Drought under global warming: a review. WIREs Clim. Change 2, 45–65.

Davies, W. J., Zhang, J., 1991. Root signals and the regulation of growth and development of plants in drying soil. Annual review of plant biology, 42(1), 55-76.

Farooq, M., Wahid, A., Kobayashi, N., Fujita, D., & Basra, S. M. A. (2009). Plant drought stress: effects, mechanisms and management. In Sustainable Agriculture (pp. 153-188). Springer Netherlands.

Flexas, J., Medrano, H. 2002. Drought-inhibition of photosynthesis in C3 plants: stomatal and non-stomatal limitations revisited. Annals of Botany 89.2 : 183-189.

Garg B.K., 2003 Nutrient uptake and management under drought: nutrient-moisture interaction, Curr. Agric. 27, 1–8.

Loreto, F., Sharkey, T., 1990. A gas- exchange study of photosynthesis and isoprene emission in Quercus rubra L. Planta, 182: 523–31.

Monson, R., Fall, R., 1989. Isoprene emission from aspen leaves. The influence of environment and relation to photosynthesis and photorespiration. Plant Physiology, 90:267–74.

Mueller RC, et al., 2005. Differential tree mortality in response to severe drought: Evidence for long-term vegetation shifts. J. Ecol. 93:1085–1093.

Nemani, R. R., Keeling, C.D, Hashimoto H., Jolly W.M., Piper S.C., Tucker C.J., Myneni R.B., Running, S.W., 2003. Climate-driven increases in global terrestrial net primary production from 1982 to 1999. Science. 300 (5625), 1560-3.

Peñuelas, J., Llusià, J., Asensio, D., Munné-Bosch, S., 2005. Linking isoprene with plant thermotolerance, antioxidants, and monoterpene emissions. Plant, Cell and Environment, 28: 278-296.

Rosenzweig, C., Iglesias, A., Yang, X. B., Epstein, P. R., & Chivian, E. 2001. Climate change and extreme weather events; implications for food production, plant diseases, and pests. Global change & human health, 2(2), 90-104.

Sharkey, T., Yeh, S., 2001. Isoprene emission from plants. Annual Review of Plant Physiology and Plant Molecular Biology, 52: 407–436.

Slatyer J. O., 1967. Plant–water relationships. Academic press, New York and London

Taiz L., Zeiger E., 2006. Plant Physiology, 4th edn., Sinauer, Massachusetts.

CHAPTER 2

Assessing gas-exchange, sap flow and water relations using tree canopy spectral reflectance indices in irrigated and rainfed *Olea europaea*

Giovanni Marino[a,b] Emanuele Pallozzi[c], Claudia Cocozza[a], Roberto Tognetti[a], Alessio Giovannelli[d], Claudio Cantini[d], Mauro Centritto[a]

[a] Dipartimento di Bioscienze e Territorio, Università degli Studi del Molise, Contrada Fonte Lappone, 86090 Pesche, IS, Italy

[b] Institute for Plant Protection, National Research Council, Via Madonna del Piano 10, 50019 Sesto Fiorentino, FI, Italy

[c] Institute of Agro-Environmental and Forest Biology, National Research Council, Via Salaria km 29.300, 00015 Monterotondo Scalo, RM, Italy

[d] Trees and Timber Institute, National Research Council, Via Madonna del Piano 10, 50019 Sesto Fiorentino, FI, Italy

Article published by *Environmental and Experimental Botany*, 99 (2014) 43–52

ABSTRACT

Diurnal and seasonal trends of leaf photosynthesis (A), stomatal conductance to water (g_s) and water potential (Ψ_l), whole-plant transpiration and tree canopy spectral reflectance indices were evaluated in rainfed and well-watered (control) mature olive (*Olea europaea* L., cv. Leccino) trees. The objective was to evaluate whether photochemical reflectance index (PRI), water index (WI) and normalized difference vegetation index (NDVI) could be used for detecting plant functioning in response to seasonal drought. The measurements were made from March to November, repeated every four weeks during the drought period of the growing season. Rainfed trees were subjected to prolonged water deficit with soil water content ranging between ~30% and 50% than that of control. Consequently, there were significant differences in the diurnal trend of Ψ_l, A, g_s and sap flux density between treatments. Under severe drought, Ψ_l ranged between ~−4.5 MPa (predawn) and ~−6.4 MPa (midday), A ranged between maximum morning values of ~6 μmol m^{-2} s^{-1} and minimum late afternoon values of 2.5 μmol m^{-2} s^{-1}, g_s

was lower than ~0.03 mol m^{-2} s^{-1} for most of the daily courses, whereas stem sap flux density reached maximum peaks of 2.1 g m^{-2} s^{-1} in rainfed plants. The diurnal trends of all these parameters fully recovered to the control level after autumn rains. PRI, NDVI, and WI of olive tree canopy assessed significantly the effects of drought on rainfed trees and their subsequent recovery. PRI resulted better correlated with A (r^2 = 0.587) than with the other measured parameters, pooling together values measured during the whole growing season. In contrast, NDVI showed a stronger relationship with Ψ_l (r^2 = 0.668) and g_s (r^2 = 0.547) than with A (r^2 = 0.435) and whole-plant transpiration (r^2 = 0.416). WI scaled linearly as g_s and Ψ_l increased (r^2 = 0.597 and r^2 = 0.576, respectively) and, even more interestingly, a good correlation was found between WI and whole-plant transpiration (r^2 = 0.668) and between WI and A (r^2 = 0.640). Overall PRI and WI ranked better than NDVI for tracking photosynthesis, whereas WI was the most accurate predictive index of plant water status and whole-plant transpiration. This study, which is the first to our knowledge that combines diurnal and seasonal trends of leaf gas-exchange, whole-plant transpiration and reflectance indices, clearly shows that PRI and WI measured at the tree canopy can be used for fast, non intrusive detection of water stress.

2.1 Introduction

Water is the most limiting resource in the Mediterranean region, where the climate is typically characterized by high potential evaporation and low and highly variable rainfall during the growing season. The agricultural sector is the largest water consumer accounting for about 70% of all extracted water (Gilbert, 2012). In the Mediterranean regions, agriculture consumes on average about 65% of total water abstraction (Simon et al., 2011). Climate change, which is increasing the chronic water scarcity in the Mediterranean basin (Dai, 2010), together with rapidly growing demand of water for industrial and urban uses, is likely to put under unprecedented pressure the limited water resources for agriculture. Therefore, the major need for development of irrigation is to save substantial water through improved irrigation management and increased water productivity (Fereres et al., 2011).

Optimization of irrigation requires the retrieval of real time crop condition and its sensitivity to water stress, which, in turn, results from specific physiological status, soil–water availability, climatic conditions (Centritto et al., 2000; Tognetti et al., 2009). Water deficit constraints all the physiological processes involved in plant growth and development. These changes are part of a cascade of responses to drought affecting primary processes including tissue water relations and gas-exchange mechanisms (Alvino et al., 1994; Magnani et al., 1996;

Aganchich et al., 2009). It is of paramount importance, consequently, to improve non-invasive phenotyping methods to monitor water relations and photosynthetic status in plants experiencing water stress (Loreto & Centritto, 2008; Centritto et al., 2009). Continuous recording of sap flow rate might provide indirect measurements of plant water status, and represent a promising tool for the development of monitoring systems in olive tree plantations to determine irrigation needs in real time, or at least at frequent intervals, and for being integrated with remote sensing techniques in precision irrigation management and control (Fernández et al., 2008).

Major progress has been made with the use of remotely sensed vegetation indices to assess physiological traits associated with plant water status (Peñuelas & Filella, 1998; Sun et al., 2008; Garbulsky et al., 2011). The methodology is based on a number of visible (Vis)- and near infrared (NIR)-based indices as indicators of photosynthetic activity (Gamon et al., 1997) and water status (Sun et al., 2008; Elsayed et al., 2011). The photochemical reflectance index, which was originally developed to estimate rapid changes in the xanthophyll (Gamon et al., 1992), is increasing used to assess changes in the efficiency of photosynthetic activity (Garbulsky et al., 2011) at different plant scale level (Gamon et al., 1997;Garbulsky et al., 2008; Naumann et al., 2008; Suárez et al., 2008). Relationships between photosynthetic parameters and PRI determined at canopy level have been reported in studies performed on grassland, sunflower, grapevine, and olive (see Garbulsky et al., 2011 for a review). Similarly, the NIR-based water index (WI) is increasingly employed for monitoring plant water status (Peñuelaset al., 1993; Peñuelas & Filella, 1998). Whereas, the normalized difference vegetation index (NDVI), which is based on different radiation absorption by green biomass in Red and NIR wavebands (Rouse et al., 1973), is widely used for the assessment of the green plant biomass at ground, airborne and satellite levels (Peñuelas & Filella, 1998). Further indications about the physiological status of plant can be obtained by the evaluation of the photosynthetic pigment composition. For this purpose, Chlorophyll Index (CI) and Structural Independent Pigment Index (SIPI) were developed to assess chlorophyll concentration and carotenoids/chlorophyll ratio, respectively (Gitelson & Merzlyak, 1994; Peñuelas & Filella, 1998).

Olive (*Olea europaea* L.) is a drought tolerant species which has been traditionally cultivated in agricultural rainfed systems in the Mediterranean basin. However, to promote olive fruit production and its economic competitiveness, there has been a large increase in the amount of irrigation water used in olive farming over the past years. To detect water needs, in order to increase water productivity through the management of precision irrigation (Fereres et al., 2011), studies have been recently performed on olive potted plants for remote sensing of water stress using rapid spectral reflectance measurements of leaf water status and photosynthetic limitations (Sun et al., 2008; Sun et al., unpublished data). In the present work, photosynthesis, whole-plant

transpiration and spectral reflectance indices were measured in mature olive trees under rainfed conditions and in irrigated control. Furthermore, the effects of water deficit on specific leaf area, pigment and nitrogen concentration were evaluated. The aim of this work was to evaluate whether PRI, WI and NDVI could track rapid changes in plant functioning also in field-grown plants subjected to seasonal drought and if CI and SIPI could detect variations occurred in pigment composition.

2.2 Materials and methods

2.2.1 Field conditions and plant material

The experiment was performed at the "Santa Paolina" experimental station of the CNR-IVALSA, located in Follonica, central Italy (42°55'58" N, 10°45'51" E, 17 m a.s.l.). The olive orchard used consisted of 10-year-old trees (*O. europaea* L., cv. Leccino) spaced at 4 × 4 m. The soil is sandy-loam (sand 64.2%, silt 16.9% and clay18.9%). The soil belongs to the Piane del Pecora system and was developed on recent alluvional deposits of river and river-pond nature. The depth of the soil was 3 m. The climate is of Mediterranean type with hot and dry seasons from April to September and cold winters. In the three growing seasons preceding the experiment, all trees were equally irrigated with micro-sprayers located 30 cm from the trunk irrigating an area of soil with a ray of 1.25 m to guarantee the uniformity of plant development. Two irrigation treatments (rainfed and well-watered control) were applied starting from mid-May of 2011. The amount of water supplied to the control trees was estimated weekly by calculating reference evapotranspiration according to the Penman-FAO equation and crop evapotranspiration (Doorenbos & Pruitt, 1977) using a crop coefficient of 0.5 as reported by Gucci (2003) for the same area and plantation. The coefficient of ground cover was 0.8, according to tree size. The volume of the irrigation water was then adjusted in order to keep predawn leaf water potential (Ψ_l) around −0.5 MPa. The irrigation period lasted from mid-May to late October 2011; each of the control trees received an average of 3900 L of water. During this period the precipitation was 125 mm with a peak on July (51.6 mm).

2.2.2 Meteorological data

Climate data were recorded every 15 min by a standard meteorological digital station placed at 100 m from the orchard (quality-controlled data were supplied by the Laboratory of monitoring and environmental modeling for the sustainable development, Florence,

http://www.lamma.rete.toscana.it/en). The variables measured were air temperature (°C), precipitations (mm) and relative humidity (RH, %).

2.2.3 Soil water content measurements

Volumetric soil moisture content was measured using Terrasense SMT2 soil moisture sensors (model PS-0077-DD, Netsens s.r.l, Florence, Italy) installed in the middle of the irrigation ray at an average distance of 90 cm from the trunk and at 10 cm and 30 cm depths in each plot. Soil moisture content was acquired every 15 min with a Netsens communication platform based on a GPRS integrated main unit, a wireless units and LiveData software for data storage and elaboration.

2.2.4 Sap flow measurements

Granier-type sensors (Granier, 1985) were inserted radially into 20 mm depth of the stem at the height of ∼1.3 m in six plants. The sensors consisted of a pair of copper-constant thermocouples of the same diameter vertically spaced of ∼15 cm. The upper probe was continuously heated through a heating wire supplied with a constant power source (120 mA). The temperature difference of the two probes was recorded to obtain the sap flux density, as derived empirically (Granier, 1987; Huang et al., 2009). Sap flux density (F_d, g H_2O m^{-2} s^{-1}) was monitored using self-made thermal dissipation probes (SF-L sensor) (Granier, 1987):

$$F_d = \alpha K^{\beta}$$

where α and β are parameter values, 119 and 1.231, respectively, and K is the dimensionless sap velocity index:

$$K = (\Delta T_{max} - \Delta T) / \Delta T$$

where ΔT_{max} is the temperature difference between the heater and reference probe at zero flow (i.e., measured predawn when F_d is assumed negligible) and ΔT is the temperature difference at any given measurement point.

2.2.5 Gas-exchange measurements

Gas-exchange measurements were made monthly from March to November 2011. Diurnal courses of photosynthesis (A) and stomatal conductance to water (g_s) were measured on five leaves for each plant. The measurements were made on the central section of a newly expanded sunny leaf using a LI-6400-40 leaf chamber fluorometer (Li-Cor, Inc., Nebraska, USA). Leaves

inside the cuvette were exposed to a flux of ambient air, with CO_2 concentration fixed at 385 μmol mol^{-1}. Air temperature and relative humidity were maintained close to ambient values. Radiation intensities, provided by a red-blue light diode source, were equal to the photosynthetic photon flux density (PPFD) levels measured at the leaf proximity with the LI-6400 PPFD sensor.

2.2.6 Leaf water potential measurements

In March, and from August to November, daily trends of leaf water potential (Ψ_l) were measured in parallel with the gas-exchange measurements. From predawn until late afternoon, five sunny-leaves per olive tree were detached from mid canopy and rapidly enclosed in a Scholander-type pressure chamber (SKPM1400, Skye Instruments, Llandrindod Wells, UK).

2.2.7 Tree spectral reflectance analysis

Simultaneously with the gas-exchange measurements, spectral reflectance of individual trees was measured by using a portable spectrometer (ASD FieldSpec 3, Analytical Spectral Devices Inc., USA), operating in the spectral range between 350 and 1025 nm with an average spectral resolution of 3 nm (Full-Width-Half-Maximum) and a sampling interval of 1.4 nm. Measurements were always made in clear weather conditions. Fiber optic cables, providing a field of view edge of 25°, were mounted on movable arms and connected to the spectroradiometer to collect reflectance spectra in nadir direction, from a distance of 1.8 m above the tree. Three measurements, taken from different fixed positions of the movable arm over each tree, were averaged to estimate the spectral response at the whole-tree scale and, thus, of the single tree canopy. The reflectance of a 1 × 1 m polystyrene panel, covered with a mixture of barium sulfate powder and white paint, was taken as white standard before every reflectance measurement (Knightonand Bugbee, 2004). Scaffolds positioned behind the shaded side of the trees were used to approach the top of the canopy to perform the measurements. ViewSpecPro (ASD) software was used to pre-processing reflectance spectra and then reflectance indices where derived.

Water Index (WI) was calculated as R_{900}/R_{970}, where R is the reflectance at the wavelength indicated in the sub-indices (Peñuelas and Filella, 1998). The narrow band version of Normalized Difference Vegetation Index (NDVI) defined by Sims and Gamon (2003) was calculated as $(R_{800} - R_{680})/(R_{800} + R_{680})$. Photochemical Reflectance Index (PRI) was calculated as $(R_{531} - R_{570})/(R_{531} + R_{570})$ (Gamon et al., 1992). Whereas Chlorophyll Index (CI) and Structural Independent Pigment Index (SIPI) were calculated to evaluate differences in

chlorophyll concentration and carotenoids/chlorophyll ratio as $(R_{750} - R_{705})/(R_{750} + R_{705})$ and $(R_{800} - R_{445})/(R_{800} - R_{680})$, respectively (Gitelson & Merzlyak, 1994; Peñuelas & Filella, 1998).

2.2.8 Specific leaf area, pigment and nitrogen concentration

Three leaves per position (higher, medium and lower part of the canopy) and per plant were collected in September, scanned with an image analyzer (UTHSCSA Image tool program, University of Texas Health Science Center, San Antonio, USA) to measure leaf area, and then oven-dried at 80 °C for 48 h to determine their dry mass. Specific Leaf Area (SLA, $m^2\ g^{-1}$) was calculated. Pigments were extracted from 0.38 cm^2 leaf discs collected with a 7 mm-diameter borer (avoiding veins) in 96% methanol solution in the dark for 96 h (Lichtenthaler, 1987). Chlorophyll *a*, chlorophyll *b* and carotenoids absorbances were determined in the methanol extract at 663, 646 and 470 nm, respectively using a UV–Vis spectrophotometer (Beckman Coulter Inc., DU 640, Indianapolis, USA). The absorbance values were converted to concentration following the procedure proposed by Lichtenthaler (1987). Approximately 1 g of leaf oven-dried and ground samples were prepared in duplicate for nitrogen analysis. N concentration was measured using the Kjeldahlmethod (Black et al., 1965).

2.2.9 Statistics

The experimental design was a complete randomized blocker plicated three times. Measurements were performed on three trees (one tree per block) per treatment. All statistical analyses were conducted using Sigma Plot 12.0 software (Systat Inc., San Jose, CA, USA) and SPSS 15.0 (SPSS Inc., Chicago, USA). Data were tested comparing treatment means using t-test. Treatment and time effects on pigment concentrations and pigment-based reflectance indices were tested using simple factorial ANOVA and repeated measures analysis of variance. Simple regressions were calculated to analyze relationship between reflectance indices and physiological parameters, determining coefficients of determination and significance levels. Regression curves were fitted to develop empirical models based on linear relationships using repeated random sub-sampling of 80% of each measured gas-exchange and water relation parameter as training data, whereas the remaining sub-sampling of 20% was retained as tested data. Then the root-mean-square error (RMSE) was calculated as a measure of the difference between the observed and the predicted values of the physiological parameters.

2.3. Results

The measurements were made in representative days of the growing season 2011, which was characterized by low amounts of rainfall accompanied by days of high air temperature and low relative humidity (Fig. 2.1 a). The diurnal courses of air temperature and relative humidity changed over the growing season. Maximum air temperature did not exceed 23°C in March (Fig. 2.1 a1) and 16°C in November (Fig. 2.1 a6), whereas air temperature reached maximum values in August and September (about 30°C). The minimum values of relative humidity (~19%) were recorded at midday in March and September (~27%). In general, the diurnal changes of both temperature and relative humidity indicate that the maximum values of vapor pressure deficit were reached between 9:00 and 17:00 during the summer months. Soil water content was strongly affected by precipitation regime from June to September (Table 2.1) and, consequently, rainfed olive trees were subjected to prolonged water deficit. In rainfed conditions, the lowest SWC values, i.e., ~30% compared to the control treatment, were recorded in June, and remained about 50% lower than those of control over the remaining summer period and at the beginning of autumn. Furthermore, significant differences in SWC at the top layer were also recorded in March and in November, despite no differences were observed between the two irrigation treatments in SWC of deeper soil layers as a result of the rains that occurred before these dates.

Table 2.1: Volumetric soil water content (SWC) of *Olea europaea* under well-watered and rainfed conditions measured at the soil depths of 10 cm and 30 cm during the growing season. Data are mean of four blocks per treatment ± SE. Asterisks indicate statistically significant differences between the two treatments (*** = $P < 0.001$, ** = $P < 0.01$).

SWC (%)						
Time	*28 March*	*22 June*	*21 July*	*24 August*	*28 September*	*16 November*
10 cm soil depth						
Control	26.18±0.35	32.13±0.43	34.24±0.45	34.84±0.47	33.51±0.45	33.73±0.41
Rainfed	18.70±0.25***	9.67±0.13***	18.36±0.24***	16.20±0.22***	14.95±0.20***	30.76±0.45**
30 cm soil depth						
Control	24.2±0.32	33.20±0.44	29.7 ±0.40	27.74±0.37	20.5 ±0.27	28.84±0.39
Rainfed	23.43±0.31	10.90±0.44***	15.6 ±0.21***	13.70±0.18***	12.56±0.17***	29.38±0.38

There were no significant differences in the diurnal trend of sap flux density between control and rainfed plants at the beginning of spring and in autumn (Fig. 2.1 b1 and b6). Furthermore, the maximum stem sap flux density reached values as low as 9.5 g m^{-2} s^{-1} in March and November

(Fig. 2.1 b1 and b6), suggesting that the weather conditions limited water loss. In contrast, the daily course of sap flux density was significantly higher ($P < 0.001$) in control than in rainfed plants over the summer period and at the onset of autumn (Fig. 2.1 b2-5). In June and July, stem sap flux density started increasing between 6:00 and 7:00 h and peaked at about 9:00–10:00 h in control plants. Then during the next four-five hours, stem sap flux density dropped progressively to minimum values which occurred at 16:00 h. This depression was then followed by a second daily maximum, reached at 18:00 h, as temperature declined and RH increased in the late afternoon. Finally, as light intensity further declined toward the end of the day also stem sap flux density dropped until whole-plant transpiration approached zero. A similar, although less pronounced trend in stem sap flux density was also recorded in August in control plants. Whereas at the beginning of autumn, stem sap flux density did not vary markedly after reaching the morning peak, indicating that there was no "midday" drop in whole-plant transpiration in control plants. The daily maximum sap flux density recorded over the summer period in control ranged between 20 and 30 g m^{-2} s^{-1}. In rainfed conditions, on the contrary, whole-plant transpiration was very low over the summer period and at the onset of autumn. Stem sap flux density showed minimum diurnal evolution in June and September (with maximum peaks of 2.6 and 2.1 g m^{-2} s^{-1}, respectively) and higher daylight evolutions in July and August, when maximum peaks of ~7 g m^{-2} s^{-1} were reached.

Similarly to the diurnal trend of sap flux density, overall significant differences in the daylight variation of photosynthesis (A) (Fig. 2.1 c) and stomatal conductance to water (g_s) (Fig. 2.1 d) between irrigation treatments were found only under drought conditions (i.e., over the summer period and at the onset of autumn). In March (Fig. 2.1 c1) and November (Fig. 2.1 c6), A reached values higher than 11 µmol $m^{-2}s^{-1}$, with little differences between the two irrigation treatments (Fig. 2.1 c1), despite g_s showed higher mean values in rainfed than in control plants in March (Fig. 2.1 d1) and very similar values in November (Fig. 2.1 d6). There were no clear indications of midday depression of both A and g_s. Whereas, as expected under drought conditions A (Fig. 2.1 c2-5) and g_s (Fig. 2.1 d2-5) dropped dramatically. A and g_s registered minimum diurnal trends in June, August and September (when maximum peaks of ~6 µmol m^{-2} s^{-1} and ~0.04 mol m^{-2} s^{-1} in A and g_s, respectively, were recorded) and higher daylight values in July, when A and g_s reached maximum values of ~10 µmol m^{-2} s^{-1} and ~0.09 mol m^{-2} s^{-1}, respectively.

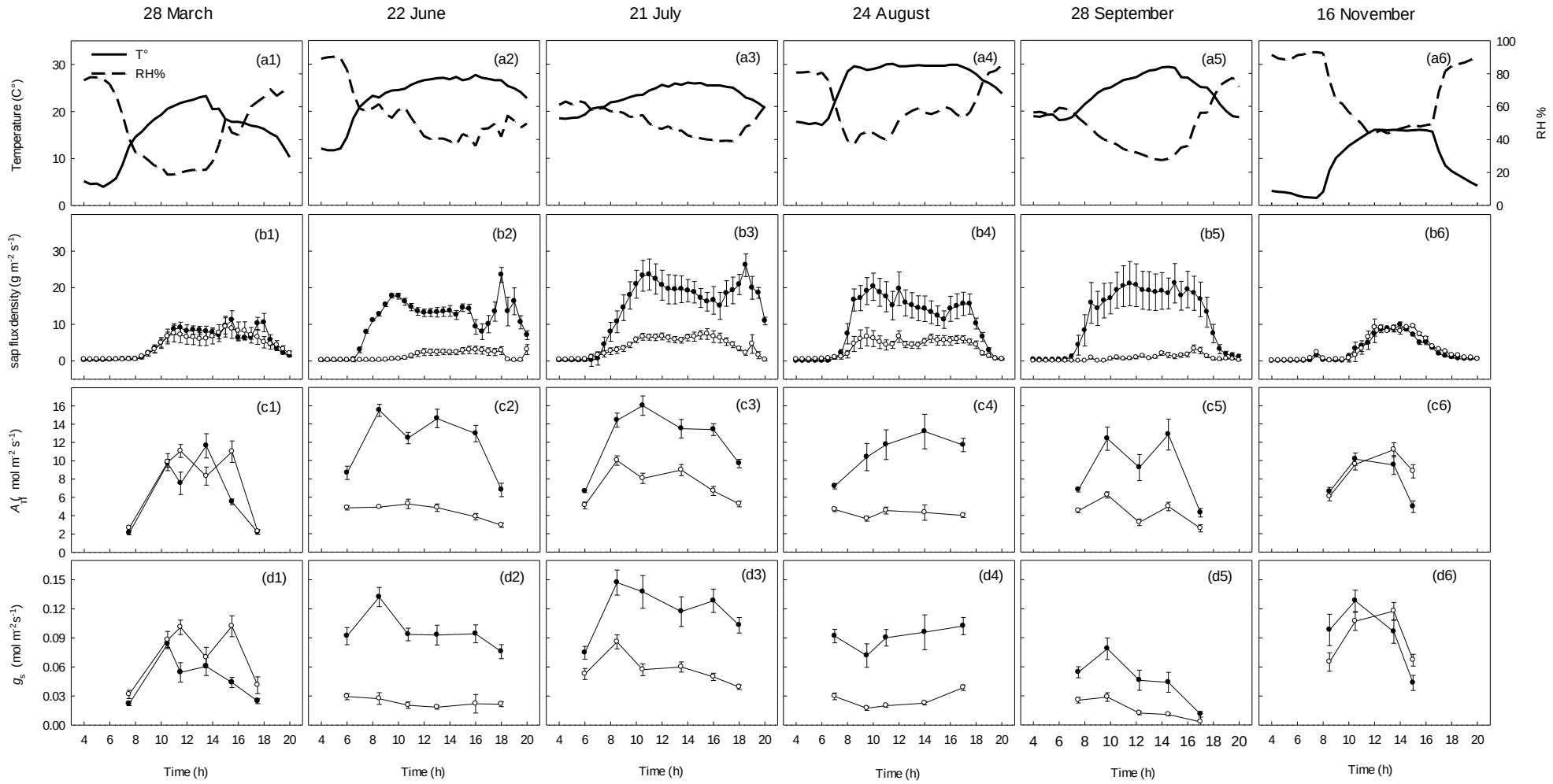

Fig. 2.1: Daily course of (a1,6) air temperature and relative humidity, (b1,6) sap flux density, (c1,6) photosynthetic rate (*A*) and (d1,6) stomatal conductance to water (g_s) measured in well-watered (●) and rainfed (○) *Olea europaea* plants during the growing season. Data are mean of three plants per treatment ± SE; *A* and g_s were measured on 5 sunny leaves per plant.

In control trees, the maximum values of A and g_s (~16 μmol m^{-2} s^{-1} and ~0.15 mol m^{-2} s^{-1}, respectively) were recorded at the beginning of summer and in July. Then, A slightly declined to maximum daily values of ~13 μmol m^{-2} s^{-1} in August and September. Whereas a marked decline in maximum g_s values was found in August (~0.10 mol m^{-2} s^{-1}) and especially in September (~0.08 mol m^{-2} s^{-1}), in correspondence of rather high diurnal air temperatures and low RH (Fig. 2.1 a4-5), and consequently high VPD values. In general, the diurnal courses of A and g_s over the summer period and at the onset of autumn showed a typical maximum in the morning followed by a declining trend in both control and rainfed plants, with the only exception of the values recorded in August which did not show any clear pattern.

The diurnal course of leaf water potential (Ψ_l) was significantly affected by time of the year and soil water availability (Fig. 2.2). In control plants, predawn Ψ_l ranged between 0.45 and 0.55 MPa over the growing season, whereas midday Ψ_l decreased on average to a minimum of about −1.6 MPa in March and November (Fig. 2.2 a and d), and to a minimum of ~−2.5 MPa in August and September (Fig. 2.2 b and c), i.e., when the evaporative demand was higher (Fig. 2.1 a). There were no significant differences in the diurnal trend of Ψ_l between control and rainfed plants at the beginning of spring (Fig. 2.2 a) and in autumn (Fig. 2.2 d), in absence of water stress. Whereas, the summer drought caused Ψ_l to decline to very low values from about −4.5 MPa predawn to a minimum of ~−6.4 MPa around midday in rainfed trees. Similarly, at the beginning of autumn predawn Ψ_l was about −3.7 MPa in rainfed trees, whereas midday Ψ_l fell below −5.1 MPa.

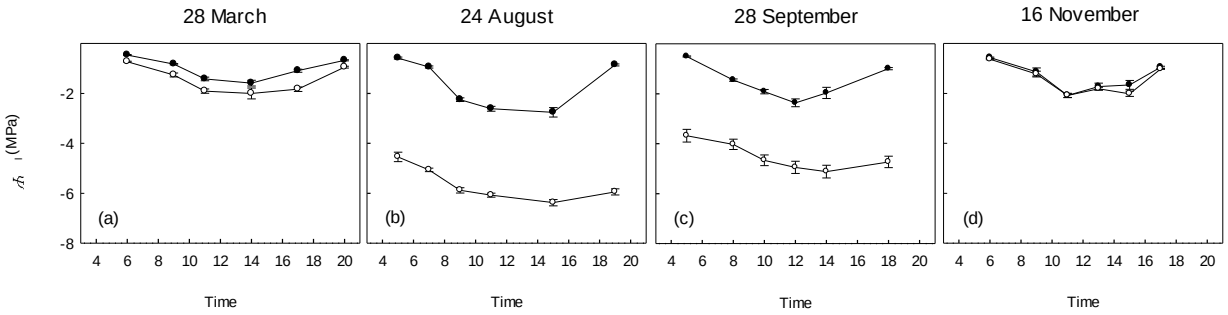

Fig. 2.2: Daily course of leaf water potential (Ψ_l) measured in well-watered (●) and rainfed (○) *Olea europaea* plants during the growing season. Data are mean of three plants per treatment (five leaves per tree) ± SE.

Leaf N concentration, which averaged about 2.9% of leaf dry mass, was not affected by irrigation treatment (data not shown). Similarly, no differences were found in SLA in response to irrigation treatment (data not shown).

Leaf pigment concentration were measured in absence of water stress (March), and toward the end of the summer drought period (September). There were no overall effects of irrigation

treatment on chlorophyll and carotenoid concentrations as well as on the carotenoid to chlorophyll *a* ratio (Tables 2.2 and 2.3). Whereas, carotenoid concentration and, consequently, the carotenoid to chlorophyll *a* ratio resulted significantly higher in September than at the beginning of the growing season. The two pigment-based canopy reflectance indices, CI and SIPI (i.e., a measure of carotenoids to chlorophyll a ratio) showed contrasting results. In fact these two indices did not show significant temporal variations (Table 2.3), whereas in September they resulted significantly affected by water stress (Table 2.2).

Table 2.2: Pigments concentrations (chlorophyll *a* – Chl *a*, total chlorophyll – Chl tot, carotenoids, carotenoid to chlorophyll *a* ratio – Car/Chl *a*) in well-watered and rainfed *Olea europaea* plants and pigment-based canopy reflectance indices (Chlorophyll Index, CI, and Structure Independent Pigments Index, SIPI) measured in March and in September. Data represent averages of three plants per treatment (nine leaves per plant sampled for pigment analysis) ± SE. Letters (a and b) indicate significant differences at $P < 0.05$ in the same column.

Time	Treatment	Chl *a* (mg mm^{-2})	Chl tot (mg mm^{-2})	Carotenoid (mg mm^{-2})	Car/Chl *a*	Chlorophyll Index	SIPI
28 March	*Control*	0.24±0.14	0.37±0.23	0.04±0.02a	0.17±0.03a	0.400±0.012ab	1.105±0.008a
	Rainfed	0.34±0.16	0.44±0.12	0.06±0.01a	0.18±0.03a	0.436±0.013 b	1.098±0.005a
28 September	*Control*	0.46±0.09	0.56±0.14	0.13±0.0 b	0.28±0.02b	0.42 ±0.015 b	1.111±0.004a
	Rainfed	0.36±0.07	0.40±0.04	0.12±0.02b	0.33±0.03b	0.363±0.020 a	1.141±0.010b

Table 2.3: Repeated measures analysis of variance for pigments concentrations (chlorophyll a - Chl a, total chlorophyll - Chl tot, carotenoids, carotenoid to chlorophyll a ratio - Car/Chl a) in well-watered and rainfed *Olea europaea* plants and pigment-based canopy reflectance indices (Chlorophyll Index, CI, and Structure Independent Pigments Index, SIPI) measured in March and in September. Significance values are indicated as ** = $P < 0.01$, * = $P < 0.05$.

Source	F statistic		
	Time	Treatment	Time x Treatment
Chl a (mg mm^{-2})	3.176 ^{ns}	0.0243 ^{ns}	1.488 ^{ns}
Chl tot (mg mm^{-2})	0.581 ^{ns}	0.217 ^{ns}	1.301 ^{ns}
Carotenoid (mg mm^{-2})	63.162 **	0.0171 ^{ns}	2.127 ^{ns}
Car/Chl a	17.844 *	0.00705 ^{ns}	1.359 ^{ns}
Chlorophyll Index	0.566 ^{ns}	1.723 ^{ns}	2.308 ^{ns}
SIPI	3.386 ^{ns}	2.415 ^{ns}	0.595 ^{ns}

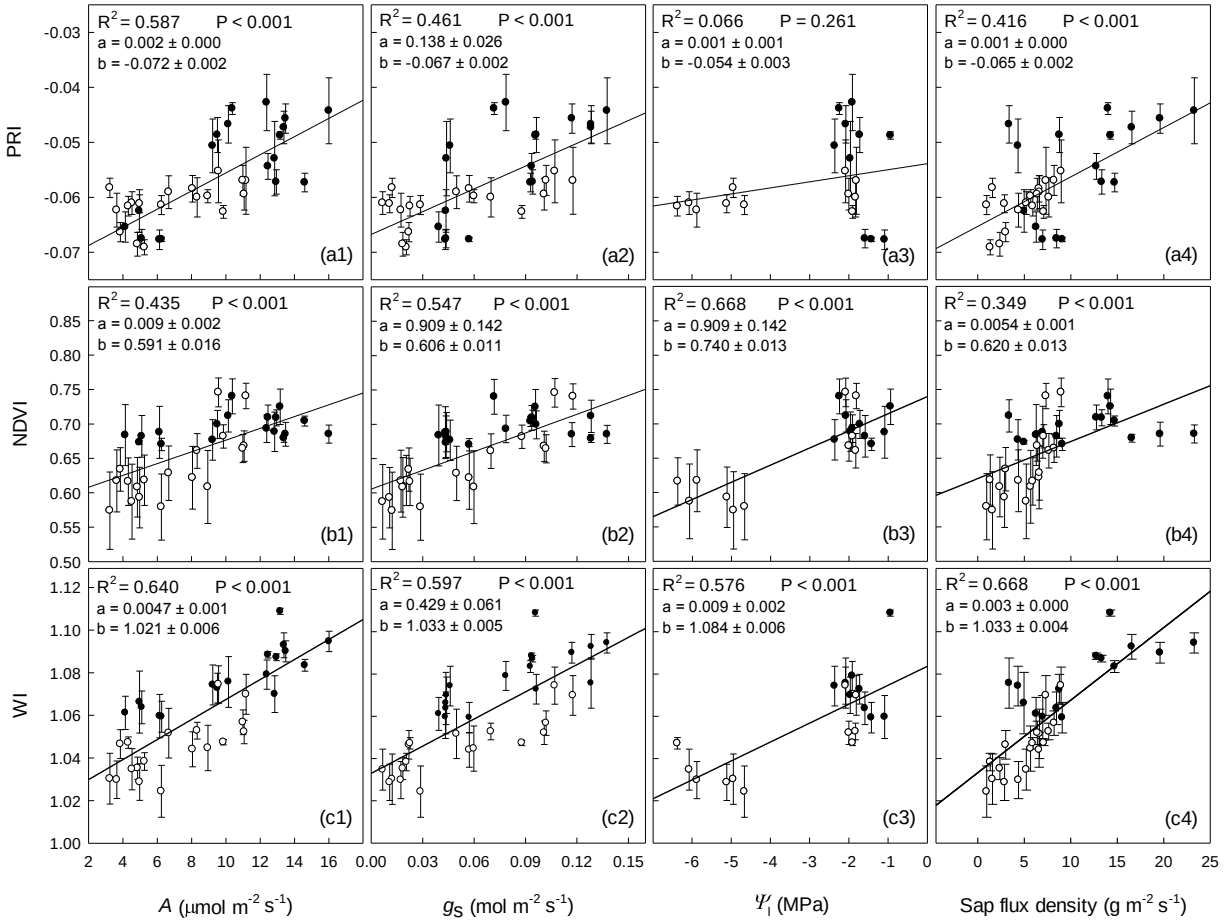

Fig. 2.3: Relationships between reflectance indices (PRI, NDVI and WI) and physiological parameters (photosynthetic rate, *A*, stomatal conductance to water, g_s, leaf water potential, Ψ_l, and sap flux density) in well-watered (●) and rainfed (○) *Olea europaea* plants during the growing season. The measurements were made between 10:00 and16.00 h. Data are mean of three plants per treatment (five leaves per tree) ± SE. The values of the slope and intercept of the linear regression functions are indicated as *a* and *b*, respectively.

Differently from gas exchange trends, spectral reflectance indices of individual tree canopy did not show any significant diurnal variation (data not shown). For this reason, to compare the physiological data with the spectral reflectance indices only data measured during the hours of maximum solar irradiation (i.e., between 10:00 and 16.00 h) were used. There were no differences in PRI, NDVI and WI between irrigation treatments in absence of water stress (March and November) (Table 2.4). Whereas, these indices were affected by drought, and resulted significantly higher in control than in rainfed trees over the summer period and at the onset of autumn. PRI resulted to be significantly linear related (r^2 = 0.587) with photosynthesis after pooling together values measured during the whole growing season (Fig. 2.3 a1). Furthermore, PRI scaled linearly also with g_s and sap flux density (Fig. 2.3 a2 and a4), although this latter relationships were weaker than the former one. In contrast NDVI showed an opposite trend, as NDVI had stronger relationships with stomatal conductance to water (r^2 = 0.547) (Fig.

2.3 b2) and above all with leaf water potential (r^2 = 0.668) (Fig. 2.3 b2) than with photosynthesis (r^2 = 0.435) (Fig. 2.3 b1).

Table 2.4: Photochemical Reflectance Index (PRI), Normalized Difference Reflectance Index (NDVI) and Water Index (WI) of *Olea europaea* under well-watered and rainfed conditions measured during the growing season. Each data represent measurements made between 10:00 and 16.00 h on individual tree canopy (at least 3 per plant) and averaged across three plants per treatment ± SE. Asterisks indicate statistically significant differences between the two treatments (*** = $P < 0.001$, ** = $P < 0.01$, * = $P < 0.05$).

Time	*28 March*	*22 June*	*21 July*	*24 August*	*28 September*	*16 November*
PRI						
Control	-0.067±0.002	-0.056±0.002	-0.046±0.004	-0.046±0.001	-0.049±0.006	-0.053±0.003
Rainfed	-0.060±0.003	-0.068±0.002***	-0.059±0.002**	-0.062±0.002***	-0.061±0.002*	-0.056±0.006
NDVI						
Control	0.68 ±0.030	0.708±0.012	0.693±0.011	0.733±0.025	0.686±0.026	0.695±0.015
Rainfed	0.669±0.021	0.620±0.037 *	0.610±0.026*	0.607±0.045*	0.582±0.039*	0.743±0.020
WI						
Control	1.061±0.008	1.086±0.002	1.09 ±0.005	1.109±0.001	1.074±0.008	1.072±0.011
Rainfed	1.052±0.004	1.040±0.005***	1.047±0.010**	1.037±0.007***	1.028±0.011**	1.072±0.009

It is noteworthy, however, that NDVI values had a high variability in water-stressed plants. Stronger linear relationships were finally found between WI and all measured parameters (Fig. 2.3 c). In fact, WI responded positively as g_s and Ψ_l increased (Fig. 2.3 c2 and c3), and stronger coefficient of determinations were found between WI and stem sap flux density (r^2 = 0.668) (Fig. 2.3 c4). In conclusion, WI assessed better than the other indices the effects of water availability on the photosynthetic activity of olive trees (r^2 = 0.640) (Fig. 2.3 c1).

All the physiological parameters estimated using the empirical algorithms obtained, are compared in Fig. 2.4 with actual measured data. Among the reflectance indices evaluated, WI shows the best accuracy in the estimation of A, g_s and mostly of sap flux density (Fig. 2.4 a3, b3 and d3). PRI allowed a sufficiently good estimate of the variation of photosynthetic rate during the growing season (Fig. 2.4 a1).

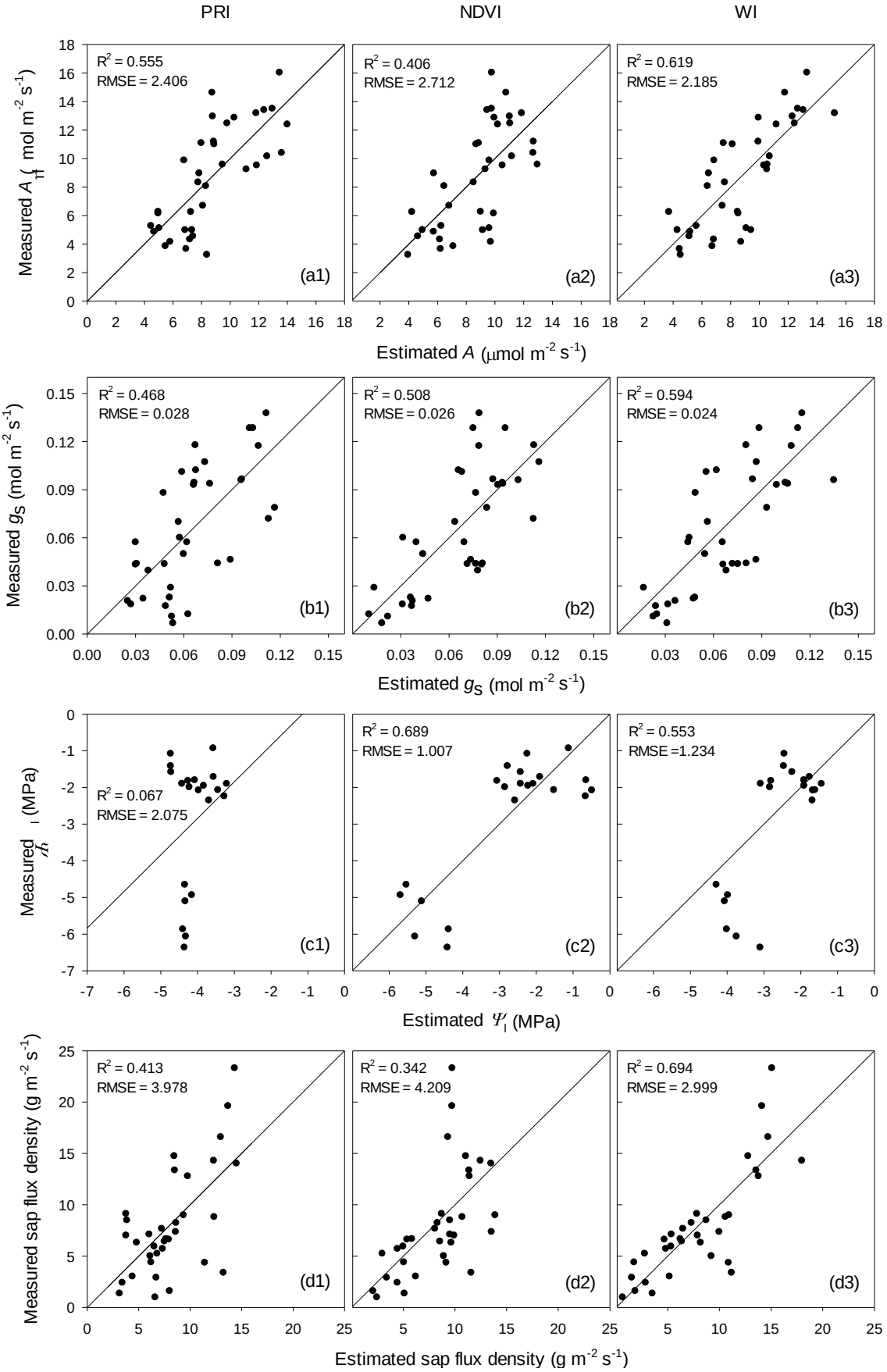

Fig. 2.4: Observed values of photosynthetic rate (A), stomatal conductance to water (g_s), leaf water potential (Ψ_l), and sap flux density versus the respective predicted values derived from the empirical relationships with PRI, NDVI and WI.

2.4 Discussion

We quantified water relations, photosynthesis and whole-plant transpiration in adult olive trees under irrigated or rainfed conditions and used spectral reflectance indices for fast monitoring of olive water status and functioning.

In our knowledge, only few studies have characterized daily and seasonal gas-exchange and water potential in olive trees in response to water deficit, both on young potted plants(Angelopoulos et al., 1996) and on mature olive trees in field conditions (Moriana et al., 2002; Diaz-Espejo et al., 2007).

Our results are overall in keeping with the findings of these previous studies. In fact, we found similar values of Ψ_l, A (Fig. 2.1 c) and g_s (Fig. 2.1 d) in both well-watered or rainfed conditions. In particular, Ψ_l (Fig. 2.2) had a typical pattern in both irrigation treatments, with a maximum values at predawn followed by a continuous decline toward midday and then by a gradual increase toward the end of the afternoon, which reflected the evaporative demand of the atmo-sphere (Fig. 2.1 a) and was modulated by water deficit (Table 2.1). In addition, in accordance with previous studies (Angelopoulos et al., 1996; Moriana et al., 2002; Diaz-Espejo et al., 2007), the daily courses of A (Fig. 2.1 c) and g_s (Fig. 2.1 d) were affected primarily by SWC (Table 2.1), and there was also a tendency to reach maximum values in the morning, as PPFD and temperature increased, followed by a midday depression and a slow declining trend in the afternoon in trees subjected to severe drought stress conditions. This is a pattern that typically occurs in trees and crops grown in Mediterranean conditions (Angelopoulos et al., 1996; Moriana et al., 2002). Furthermore, the rainfed values recorded under severe water stress of Ψ_l, which ranged between ∼−4.5 MPa (predawn) and ∼−6.4 MPa (midday) (Fig. 2.2), photosynthesis, which ranged between maximum morning values of ∼6 μmol m^{-2} s^{-1} and minimum late afternoon values of 2.5 μmol m^{-2} s^{-1} (Fig. 2.1 c) despite g_s was lower than ∼0.03 mol m^{-2} s^{-1} for most of the daily courses (Fig. 2.1 d), are a further indication that olive trees are able to tolerate severe drought stress conditions. Angelopoulos et al. (1996) showed that the declined in A under severe water stress was caused by a combination of both stomatal and metabolic limitations. Furthermore, Moriana et al. (2002) found that photosynthesis of severely water-stressed olive trees did not recover to the control level with the autumn rains, implying that A was impaired by non-diffusional limitations (Centritto et al.,2005; Diaz-Espejo et al., 2007; Aganchich et al., 2009). Impaired carbon metabolism usually follows CO_2 transport limitations when environmental stress becomes severe (Cornic, 2000; Centritto et al., 2003). Thus, despite A of rainfed plants fully recovered to the control level after the autumn rains (Fig. 2.1 c6), it is likely that some degree of metabolic limitations took place under severe

drought when g_s fell well below ~0.03 mol m^{-2} s^{-1} (Fig. 2.1 d2,5), indicating that the amount of soil water available to support plant transpiration was extremely limited (Centritto et al., 2011a). The good correspondence between g_s, Ψ_l and SWC across treatments suggested that olive trees were able to restrict, at least partially, water loss by closing stomata. The difference between predawn and midday Ψ_l tended to increase with decreasing soil water availability (and soil water potential) because of a combination of moderate stomatal regulation of transpiration rate and the usually higher transpiration demand in drier periods. Indeed, these olive trees presented anisohydric behavior in relation to soil drought. Anisohydric species tend to occupy more drought-prone habitats compared with isohydric species and have xylem that is more resistant to negative water potential (Centritto et al., 2011b).Olive tree water use was likely to be largely controlled by the diffusion or adiabatic term of the Penman–Monteith equation for evapotranspiration, the transpiration being strongly coupled with the surrounding air (namely VPD) and radiation environment. Diurnal sap flow patterns showed a step morning increase, more evident under good soil moisture conditions, probably related to woody tis-sues water capacitance (Tognetti et al., 2009). Nevertheless, water stored in woody tissues was not sufficient to maintain transpiration in rainfed trees, and sap flow diurnal patterns showed a pronounced reduction throughout summer (Fig. 2.1 b). This reflected soil water depletion without supplement irrigation, which was, instead, effective in countering water deficit in control trees, at least under these experimental conditions. However, a decline of diurnal sap flow patterns during the season in irrigated trees may be expected due to high water depletion of soil portions explored by roots (Tognetti et al., 2004, 2005; Fernández et al., 2008).The detection of plant functioning by assessing associated spec-tral indices has been a major focus of remote sensing (Gamon et al., 1992; Peñuelas & Filella, 1998; Sun et al., 2008; Garbulsky et al., 2011; Tsonev et al., 2013). Sun et al. (2008) found that water stress caused significant changes in the spectral reflectance, in the Vis and NIR regions, of leaves of potted olive plants. They found that a 15-day water stress cycle significantly affected PRI and indices that used algorithms based on the 1455 nm wavelength, whereas WI and SIPI were not significantly affected. PRI, which is a Vis-based index originally elaborated to estimate xanthophyll cycle pigments (Gamon et al., 1992, 1997) and carotenoid/chlorophyll ratios (Sims & Gamon, 2002), has been shown to adequately track photosynthetic activity (see Garbulsky et al., 2011) also under water stress conditions (Sarlikioti et al., 2010; Ripullone et al., 2011; Tsonevet al., 2013). In accordance with these studies, PRI of olive tree canopy was significantly affected by drought in the rainfed treatment (Table 2.4). Furthermore, NDVI, an index widely used for the assessment of a larger number of plant and ecosystem proper-ties (Ollinger, 2011), and WI, which is extensively used to assess g_s and leaf water status (Peñuelas et al., 1993; Serrano et al., 2000; Gutierrez et al.,

2010), estimated at the canopy level, were significantly modified in rainfed plants subjected to drought stress(Table 2.4). This is in keeping with a recent study (Serrano et al., 2010) which showed that both NIR-based NDVI and WI are good indicators of vineyard water status. However, our results are in contrast with WI estimated on detached leaves of water-stressed olive saplings grown in pots (Sun et al., 2008). Experimental design and measurement methodology, may account for these conflicting results. The diurnal courses of PRI, WI, and NDVI of the olive tree canopy were not significant (data not shown). The lack of responsiveness of these indices to the low radiation levels recorded I the early morning and late afternoon hours has been reported to be related to the bi-directional reflectance distribution function (Suárez et al., 2008; Sarlikioti et al., 2010). Thus, to correlate reflectance indices to the gas-exchange and water status parameters, the values obtained from early morning and late afternoon were discarded. The good linear relationship between canopy PRI and leaf photosynthesis (Fig. 2.3 a1) confirms the results found on detached leaves of olive saplings grown in pots under water deficit conditions (Sun et al., unpublished data). There is a growing body of literature showing that PRI is correlated with photosynthetic parameters (Garbulsky et al., 2011). Moreover, recent studies have shown significant correlations between PRI and carbon assimilation in different plant species subjected to water stress conditions, for instance in greenhouse-grown *Solanum lycopersicum* (Sarlikiotiet al., 2010), and in pot-grown Mediterranean evergreen seedlings of *Quercus ilex* and *Arbutus unedo* (Ripullone et al., 2011), and *Ceratonia siliqua* (Osório et al., 2012). NDVI resulted to be less reliable than PRI to remotely assess the photosynthetic rate in Olive trees (Fig. 2.4 a1 and a2). In fact, NDVI is known to be sensitive to fractional PAR intercepted by green biomass, but it is not always a reliable tool to assess variations in photosynthetic radiation-use efficiency that can occur seasonally without a substantial alteration of canopy greenness (Gamon et al., 1995). On the other hand, PRI is more closely linked to photochemical performances of leaves, revealing short-term changes in de-epoxidation state of xanthophylls, a PSII light-use efficiency indicator (Gamon et al., 1997). A more reliable correlation was found between canopy NDVI and leaf g_s (Fig. 2.3 b2),and a slight better one emerged between canopy WI and leaf g_s (Fig. 2.3 c2). These results confirm early findings by Serrano et al. (2010) who showed that in general both NDVI and WI, measured at the canopy level, tracked leaf water status in grapevines, and that WI was in particular well correlated with g_s. We also found a close correlation between tree canopy WI and *A* (Fig. 2.3 c1) and, even more interestingly, between tree canopy WI and whole-plant transpiration as assessed by stem sap flux density (Fig. 2.3 c4). Over-all, our study clearly show that the spectral vegetation indices PRI,NDVI and WI measured at the tree canopy are good stress indicators that can be used for fast, nonintrusive detection of water stress. Furthermore, these results show that PRI ranks better

than NDVI for tracking photosynthesis, whereas WI is the most accurate predictive index of plant water status, whole-plant transpiration and also of the decline of photosynthetic rate in olive trees affected by water deficit. Finally, more intense, daily and seasonally, parallel measurements of physiological parameters and reflectance indices, made during the maximum solar irradiation hours, may further refine the quality of their correlations. Finally, SIPI and CI, i.e., the pigment-based reflectance indices (Peñuelas and Filella, 1998; Ollinger, 2011), resulted also sensitive to water stress (Table 2.2). However, CI and SIPI did not track either the response of both chlorophyll concentrations and carotenoid to chlorophyll *a* ratio to water stress (Table 2.2) or the temporal variation of carotenoid concentration and carotenoid to chlorophyll ratio (Table 2.3). These results, consequently, do not provide positive evidence on the reliability of such pigment-based indices. A lacks of sensitivity of SIPI for low values of carotenoid/chlorophyll ratio at canopy scale and an increasing variability for higher values of the ratio has been already described (Blackburn, 1998). A wider range of variation of pigment composition and a greater number of observations should be evaluated to better test the sensitivity of these indices. In conclusion, olive is becoming a strategic crop worldwide, and its plantation is increasingly irrigated to intensify fruit production. In order to save irrigation water and increase its productivity, there is a pressing need to monitor plant water status and functioning to detect signs and degree of water stress. Our study, performed on mature olive plantation in arid Mediterranean environment, it is the first to our knowledge that combines diurnal and seasonal trends of leaf gas-exchange, whole-plant transpiration and tree canopy reflectance indices. Our findings demonstrate that: (a) the seasonal courses of PRI, WI, and NDVI were significantly affected by drought; (b) overall these three indices scaled linearly withgas-exchange parameters; (c) PRI resulted better correlated with photosynthesis than NDVI, whereas WI was the most accurate predictive index of A, g_s, Ψ_l and whole-plant transpiration as assessed by stem sap flux density. Thus, this study shows that remotely sensed reflectance indices, in particular PRI and WI, are promising predictive tools of the impact of drought on photosynthetic activity, water status and whole-plant transpiration.

References

Aganchich, B., Wahbi, S., Loreto, F., Centritto, M., 2009. Partial root zone drying: regulation of photosynthetic limitations and antioxidant enzymatic activities in young olive (*Olea europaea*) saplings. Tree Physiol. 29, 685–696.

Alvino, A., Centritto, M., De Lorenzi, F., 1994. Photosynthesis response of sunlit and shade pepper (Capsicum annum) leaves at different positions in the canopy under two water regimes. Aust. J. Plant Physiol. 21, 377–391.

Angelopoulos, K., Dichio, B., Xiloyannis, C., 1996. Inhibition of photosynthesis in olive trees (*Olea europaea* L.) during water stress and rewatering. J. Exp. Bot. 47,1093–1100.

Black, C.A., Evans, D.D., White, J.L., Ensminger, L.E., Clark, F.E., 1965. Methods of SoilAnalysis: Part 2. Chemical and Microbial Properties. Agronomy Series, No. 9.American Society of Agronomy, Madison, WI.

Blackburn, G.A., 1998. Quantifying chlorophylls and carotenoids at leaf and canopy scales: an evaluation of some hyperspectral approaches. Remote Sens. Environ.66, 273–285.

Centritto, M., Brilli, F., Fodale, R., Loreto, F., 2011a. Different sensitivity of isopreneemission, respiration, and photosynthesis to high growth temperature coupled with drought stress in black poplar (*Populus nigra*). Tree Physiol. 31, 275–286.

Centritto, M., Lauteri, M., Monteverdi, M.C., Serraj, R., 2009. Leaf gas-exchange, carbon isotope discrimination, and grain yield in contrasting rice genotypes subjected to water deficits during the reproductive stage. J. Exp. Bot. 60, 2325–2339.

Centritto, M., Loreto, F., Chartzoulakis, K., 2003. The use of low [CO2] to estimate diffusional and non-diffusional limitations of photosynthetic capacity of salt-stressed olive saplings. Plant Cell Environ. 26, 585–594.

Centritto, M., Loreto, F., Massacci, A., Pietrini, F., Villani, M.C., Zacchini, M., 2000. Improved growth and water use efficiency of cherry saplings under reduced light intensity. Ecol. Res. 15, 385–392.

Centritto, M., Tognetti, R., Leitgeb, E., Strelcová, K., Cohen, S., 2011b. Above ground processes: anticipating climate change influences. In: Bredemeier, M., Cohen, S.,Godbold, D.L., Lode, E., Pilcher, V., Schleppi, P. (Eds.), Forest Management and the Water Cycle: An Ecosystem-Based Approach. Ecological Studies, vol. 212.Springer, Berlin, pp. 31–64.

Centritto, M., Wahbi, S., Serraj, R., Chaves, M.M., 2005. Effects of partial root zone drying (PRD) on adult olive tree (*Olea europaea*) in field conditions under arid climate: II. Photosynthetic responses. Agric. Ecosyst. Environ. 106, 303–311.

Cornic, G., 2000. Drought stress inhibits photosynthesis by decreasing stomatal aperture - not by affecting ATP synthesis. Trends Plant Sci. 5, 187–188.

Dai, A., 2011. Drought under global warming: a review. WIREs Clim. Change 2, 45–65.

Diaz-Espejo, A., Nicolas, E., Fernández, J.E., 2007. Seasonal evolution of diffusional limitations and photosynthetic capacity in olive under drought. Plant Cell Environ. 30, 922–933.

Doorenbos, J., Pruitt, W.O., 1977. Guidelines for Predicting Crop Water Requirements. Irrigation Drainage Paper, vol. 24. FAO, Rome.

Elsayed, S., Mistele, B., Schmidhalter, U., 2011. Can changes in leaf water potential be assessed spectrally? Funct. Plant Biol. 38, 523–533.

Fereres, E., Orgaz, F., Gonzalez-Dugo, V., 2011. Reflections on food security underwater scarcity. J. Exp. Bot. 62, 4079–4086.

Fernández, J.E., Green, S., Caspari, H.W., Diaz-Espejo, A., Cuevas, M.V., 2008. The use of sap flow measurements for scheduling irrigation in olive, apple and Asian pear trees and in grapevines. Plant Soil 305, 91–104.

Gamon, J.A., Peñuelas, J., Field, C.B., 1992. A narrow-waveband spectral index that tracks diurnal changes in photosynthetic efficiency. Remote Sens. Environ. 41,35–44.

Gamon, J.A., Field, C.B., Goulden, M.L., Griffin, K.L., Hartley, A.E., Joel, G., Peñuelas, J., Valentini, R., 1995. Relationships between NDVI, canopy structure, andphotosynthesis in three Californian vegetation types. Ecol. Appl. 5 (1), 28–41.

Gamon, J.A., Serrano, L., Surfus, J.S., 1997. The photochemical reflectance index: an optical indicator of photosynthetic radiation use efficiency across species, functional types, and nutrient levels. Oecologia 112, 492–498.Garbulsky, M.F.,

Peñuelas, J., Gamon, J.A., Inoue, Y., Filella, I., 2011. The Photochemical Reflectance Index (PRI) and the remote sensing of leaf, canopy and ecosystem radiation use efficiencies: a review and meta-analysis. Remote Sens. Environ.115, 281–297.

Garbulsky, M.F., Peñuelas, J., Papale, D., Filella, I., 2008. Remote estimation of carbon dioxide uptake by a Mediterranean forest. Glob. Change Biol. 14, 2860–2867.

Gilbert, N., 2012. Water under pressure. Nature 483, 256–257.Gitelson, A., Merzlyak, M.N., 1994. Spectral reflectance changes associated with autumn senescence of *Aesculus hippocastanum* L. and *Acer platanoides* L. leaves. Spectral features and relation to chlorophyll estimation. J. Plant Physiol. 143,286–292.

Granier, A., 1985. A new method of sap flow measurement in tree stems. Ann. Forest Sci. 42, 193–200.

Granier, A., 1987. Evaluation of transpiration in a Douglas fir stand by means of sapflow measurements. Tree Physiol. 3, 309–319.

Gutierrez, M., Reynolds, M.P., Klatt, A.R., 2010. Association of water spectral indices with plant and soil water relations in contrasting wheat genotypes. J. Exp. Bot.61, 3291–3303.

Gucci, R., 2003. L'irrigazione in olivicoltura. Quaderni ARSIA-Toscana, Firenze.

Huang, Y.Q., Zhao, P., Zhang, Z.F., Li, X., He, C.X., Zhang, R.Q., 2009. Transpiration of *Cyclobalanopsis glauca* (syn. *Quercus glauca*) stand measured by sap-flow method in a karst rocky terrain during dry season. Ecol. Res. 24, 791–801.

Knighton, N., Bugbee, B., 2004. A Mixture of Barium Sulfate and White Paint is a Low Cost Substitute for Spectralon, Available at: http://www.usu.edu/ cpl/PDF/BariumSulfate.pdf.

Lichtenthaler, H.K., 1987. Chlorophylls and carotenoids: pigments of photosynthetic biomembranes. Methods Enzymol. 148, 350–382.

Loreto, F., Centritto, M., 2008. Leaf carbon assimilation in a water-limited world. Plant Biosyst. 142, 154–161.

Magnani, F., Centritto, M., Grace, J., 1996. Measurement of apoplasmic and cell-to-cell components of root hydraulic conductance by a pressure-clamp technique. Planta 199, 296–306.

Moriana, A., Villalobos, F.J., Fereres, E., 2002. Stomatal and photosynthetic responses of olive (*Olea europaea* L.) leaves to water deficits. Plant Cell Environ. 25,395–405.

Naumann, J.C., Young, D.R., Anderson, J.E., 2008. Leaf chlorophyll fluorescence, reflectance, and physiological response to freshwater and saltwater flooding in the evergreen shrub Myrica cerifera. Environ. Exp. Bot. 63, 402–409.

Ollinger, S.V., 2011. Sources of variability in canopy reflectance and the convergent properties of plants. New Phytol. 189, 375–394.

Osório, J., Osório, M.L., Romano, A., 2012. Reflectance indices as non destructive indicators of the physiological status of *Ceratonia siliqua* seedlings under varying moisture and temperature regimes. Funct. Plant Biol. 39,588–597.

Peñuelas, J., Filella, I., 1998. Visible and near-infrared reflectance techniques for diagnosing plant physiological status. Trends Plant Sci. 3, 151–156.

Peñuelas, J., Filella, I., Serrano, L., Biel, C., Save, R., 1993. The reflectance at the 950-970 nm region as an indicator of plant water status. Int. J. Remote Sens. 14,1887–1905.

Simonet, S., 2011. Adapting to Climate Change in Water Sector in the Mediterranean: Situation and Prospects. Blue Plan Papers 10. Plan Bleu, Valbonne.

Ripullone, F., Rivelli, A.R., Baraldi, R., Guarini, R., Guerrieri, R., Magnani, F., Peñuelas,J., Raddi, S., Borghetti, M., 2011. Effectiveness of the photochemical reflectance index to track photosynthetic activity over a range of forest tree species and plant water statuses. Funct. Plant Biol. 38, 177–186.

Rouse Jr., J.W., Haas, R.H., Schell, J.A., Deering, D.W., 1973. Monitoring vegetation systems in the Great Plains with ERTS. Washington, DC. In: Freden, S.C., Mercanti, E.P., Becker, M.

(Eds.), Third Earth Resources Technology Satellite-1 Sympo-sium. Technical Presentations, Section A, vol. I. National Aeronautics and SpaceAdministration (NASA SP-351), pp. 309–317.

Sarlikioti, V., Driever, S.M., Marcelis, L.F.M., 2010. Photochemical reflectance index as a mean of monitoring early water stress. Ann. Appl. Biol. 157, 81–89.

Serrano, L., González-Flor, C., Gorchs, G., 2010. Assessing vineyard water status using the reflectance based water index. Agric. Ecosyst. Environ. 139, 490–499.

Serrano, L., Ustin, S.L., Roberts, D.A., Gamon, J.A., Peñuelas, J., 2000. Deriving water content of chaparral vegetation from aviris data. Remote Sens. Environ. 74,570–581.

Sims, D., Gamon, J., 2002. Relationships between leaf pigment content and spectral reflectance across a wide range of species, leaf structures and developmental stages. Remote Sens. Environ. 81, 337–354.

Sims, D., Gamon, J., 2003. Estimation of vegetation water content and photosynthetic tissue area from spectral reflectance: a comparison of indices based on liquid water and chlorophyll absorption features. Remote Sens. Environ. 84,526–537.

Suárez, L., Zarco-Tejada, P.J., Sepulcre-Cantó, G., Pérez-Priego, O., Miller, J.R.,Jiménez-Muñoz, J.C., Sobrino, J., 2008. Assessing canopy PRI for water stress detection with diurnal airborne imagery. Remote Sens. Environ. 112,560–575.

Sun, P., Grignetti, A., Liu, S., Casacchia, R., Salvatori, R., Pietrini, F., Loreto, F., Centritto, M., 2008. Associated changes in physiological parameters and spectral reflectance indices in olive (*Olea europaea* L.) leaves in response to different levels of water stress. Int. J. Remote Sens. 29, 1725–1743.

Tognetti, R., Giovannelli, A., Lavini, A., Morelli, G., Fragnito, F., d'Andria, R., 2009. Assessing environmental controls over conductances through the soil-plant-atmosphere continuum in an experimental olive tree plantation of southern Italy. Agric. Forest Meteorol. 149, 1229–1243.

Tognetti, R., d'Andria, R., Morelli, G., Alvino, A., 2005. The effect of deficit irrigation on seasonal variations of plant water use in *Olea europaea* L. Plant Soil 273, 139–155.

Tognetti, R., d'Andria, R., Morelli, G., Calandrelli, D., Fragnito, F., 2004. Irrigation effects on daily and seasonal variations of trunk sap flow and leaf water relations in olive trees. Plant Soil 263, 249–264.

Tsonev, T., Wahbi, S., Sun, P., Sorrentino, G., Centritto, M., 2013. Gas exchange, water relations and their relationships with photochemical reflectance index in *Quercus ilex* plants during water stress and recovery. Int. J. Agric. Biol. (in press).

CHAPTER 3

Photochemical reflectance index as an indirect estimator of foliar isoprenoid emissions at the ecosystem level

Josep Peñuelas[1,2], Giovanni Marino[3,4], Joan Llusia[1,2], Catherine Morfopoulos[1,2,5], Gerard Farré-Armengol[1,2], Iolanda Filella[1,2]

[1] CSIC, Global Ecology Unit CREAF-CEAB-UAB, Cerdanyola del Valle´s, Barcelona 08193, Catalonia, Spain.
[2] CREAF, Cerdanyola del Vallés, Barcelona, 08193,Catalonia, Spain.
[3] Dipartimento di Bioscienze e Territorio, Università degli Studi del Molise, Contrada Fonte Lappone, 86090 Pesche (IS), Italy.
[4] Institute for Plant Protection, National Research Council, Via Madonna del Piano 10, Sesto Fiorentino (FI), Florence 50019 , Italy.
[5] Division of Ecology and Evolution, Imperial College, Silwood Park, Ascot, London SL5 7PY, UK.

ABSTRACT

Terrestrial plants re-emit around 1–2% of the carbon they fix as isoprene and monoterpenes. These emissions have major roles in the ecological relationships among living organisms and in atmospheric chemistry and climate, and yet their actual quantification at the ecosystem level in different regions is far from being resolved with available models and field measurements. Here we provide evidence that a simple remote sensing index, the photochemical reflectance index, which is indicative of light use efficiency, is a good indirect estimator of foliar isoprenoid emissions and can therefore be used to sense them remotely. These results open new perspectives for the potential use of remote sensing techniques to track isoprenoid emissions from vegetation at larger scales. On the other hand, our study shows the potential of this photochemical reflectance index technique to validate the availability of photosynthetic reducing power as a factor involved in isoprenoid production.

Article published by *Nature Communications* 4:2604 (2013) DOI: 10.1038/ncomms3604

3.1 Introduction

Isoprene and monoterpenes (a diverse group of molecules made up of two isoprene units) are biogenic volatile organic compounds (BVOC) emitted from vegetation and are of great importance in plant biology and ecology as well as in atmospheric chemistry and climate (Peñuelas & Llusia, 2013; Peñuelas & Staudt, 2013). Total BVOC emissions are estimated to be around 1 Pg C a^{-1}, of which isoprene and monoterpenes represent more than half (Guenter et al., 2006; Arneth et al., 2008). These emissions of volatile isoprenoids have a significant effect on the atmospheric content of greenhouse gases and pollutants and secondary organic aerosols (Arneth et al., 2010; Carslaw et al., 2010), and thus also on climate (Peñuelas & Llusia, 2013; Peñuelas & Staudt, 2013; Pacifico et al., 2009).

Isoprenoid emissions at the foliar, canopy and regional level are generally estimated using models based on leaf emission capacities (E_c), which are emission rates measured at the leaf level under standard light and temperature conditions (Guenther et al. 1995; Niinemets et al., 2010a, 2010b). Temporal and spatial variations in emissions are derived by modifying E_c using empirical equations that describe the observed short-term controls based on temperature and light, and long-term controls based on antecedent weather conditions and environmental and biotic stresses (Guenter et al., 1995, 2006; Niinemets et al., 2010a, 2010b). E_c were initially considered to be species specific constants. There is now multiple evidence showing that E_c values are very variable and acclimate seasonally and over environmental gradients (Niinemets et al., 2010a, 2010b). These models are now increasing in complexity in order to manage these variations in E_c empirically (Monson et al., 2012); they use empirical functions to describe the relationships between emission rates, environmental variables and serial multipliers based on single-factor relationships in order to account for co-variations of environmental variables that improve the estimates. However, these estimates remain (Monson et al., 2012). Current efforts are now being made to base the modelling on a fundamental understanding of plant biology (Monson et al., 2012; Morfopoulus et al., in press), nevertheless, uncertainty remains high (Guenter et al., 2006; Monson et al., 2012; Morfopoulus et al., in press). For example, MEGAN isoprene flux estimates were within a factor of 2 above-canopy fluxes measured over a growing season in northern Michigan (Guenter et al., 2006).

Emissions and BVOC budgets can also be estimated by inverse modelling based on atmospheric concentrations (Karl et al. 2003; Stavrakou et al., 2009), but the actual ground and aircraft measuring of atmospheric concentrations remains both laborious and sporadic. In addition to estimates based on modelling, isoprenoid emissions can be directly measured at the canopy level by applying eddy-covariance techniques (Westberg et al., 2001; Spirig et al., 2005;

McKinney et al., 2011); this is currently the only direct way to measure BVOC flux of whole ecosystems with a high temporal resolution. However, these measurements are scarce and limited to a few small sites. Eddy-covariance techniques applied from towers can be effectively used to measure only a single 'point' over a flat and uniform terrain, usually in the order of a few hundred or thousand square meters. When applied from aircraft, eddy-covariance techniques can be used to measure several sites (Misztal et al., 2013), but studies are few in number and temporally very limited.

The spatial and temporal extension of isoprenoid flux assessment can be provided by the application of remote sensing techniques. Indirect approaches exist for the remote sensing of isoprenoid emissions through the detection of one of its oxidation products: formaldehyde (for example refs Morfopoulus et al., in press; Barkley et al., 2008). This approach relies on assumptions associated with the oxidant chemistry relating isoprenoids to formaldehyde that are subject to significant uncertainties (Barkley et al., 2008). Isoprenoid emissions can also be remotely sensed indirectly through detectable changes in carotenoid concentrations that are related to isoprenoid emissions (Owen et al., in press). Detecting BVOC exchange using remote sensing techniques is, however, a very challenging goal, and one that is far from being accomplished.

Here, our aim is to determine a simple remote sensing approach that extends our ability to assess isoprenoid fluxes in space and time. We assume a negative relationship between light use efficiency (LUE; here calculated as the ratio between measured net photosynthetic rates and incident photosynthetic photon flux density (PPFD) in mol CO_2 mol per photons) and isoprenoid emissions as a result of a higher availability of photosynthetic reducing power and substrate for isoprenoid production under lower LUEs (Peñuelas & Llusia, 2004; Owen & Peñuelas, 2005). The photochemical reflectance index (PRI), which is calculated as $(R_{531} - R_{570})/(R_{531} + R_{570})$, where R_n is the reflectance of the leaf at n nm, is a good estimator of LUE at the leaf, canopy and ecosystem levels (Gamon et al., 1992; Peñuelas et al., 1995, 2011; Filella et al., 1996; Garbulsky et al., 2011). We, therefore, hypothesize that PRI would also be useful as an estimator of isoprenoid emissions. We test our hypothesis on saplings of a deciduous species, *Populus nigra* L., an isoprene emitter, and an evergreen species, *Quercus ilex* L., which is mostly a monoterpene emitter. We calculate light-response curves for isoprenoid emissions from 0–2500 $mmolm^{-2}$ s^{-1} in leaves of saplings growing under well-irrigated conditions, under drought conditions and under conditions of senescence, and in all cases compare growth in full sun with shade, that is, we generate a wide range of LUEs to test our hypothesis. The results provide evidence that PRI is a good indirect estimator of foliar isoprenoid emissions and can therefore be

used to sense them remotely. The results also show the potential of this PRI technique to validate the availability of photosynthetic reducing power as a factor involved in isoprenoid production.

3.2 Material and Methods

3.2.1 Plant material and experimental setup

We used 4-year-old potted *P. nigra* L.and *Q. ilex* L. plants grown in a nursery (Tres Turons S.C.P., Castellar del Vallés, Catalonia, Spain), maintained under Mediterranean ambient conditions outdoors (five saplings of each species grown under sunny conditions and five saplings grown under shade conditions). They were grown in 15 L pots with a substrate composed of peat and sand (2:1). To widen the range of tested LUE conditions, an additional plant treatment was established. Irrigation was withheld from these saplings grown under sunny and shaded conditions and, after 10–15 days, they were measured again (droughted plants). In order to further widen the range of tested LUE conditions for the control, *P. nigra* saplings grown in both sunny and shaded conditions were also measured in November when the leaves were senescing (senescing leaves).

Three plants were measured per treatment. For each measurement, a small leaf chamber was clamped to a leaf. This leaf cuvette was part of a LCpro+ photosynthesis system (ADC BioScientific, Herts, England), which recorded photosynthesis (net CO2 uptake), stomatal conductance, air humidity and temperature data, while controlling light and the flow of air entering the leaf cuvette. A light-response curve was programmed into the leaf chamber, ranging from 0 to 2,500 $\mu molm^{-2}\ s^{-1}$ of PAR (Fig. 3.4); measurements were made continuously for 45 min at each light intensity and at a constant temperature of 30 °C.

3.2.2 Plant reflectance measurements

The reflectance of the clamped leaf was simultaneously measured with a UniSpec Spectral Analysis System/Reflectometer (PP Systems, Haverhill, MA, USA) operated using a palmtop PC. Fifty scans were integrated (integration time 10 ms) per sample. Reflectance measurements were preceded by a dark scan and compared with reflectance measurements from a Spectralon (Labsphere, North Sutton, NH, USA) white standard in order to obtain the reflectance values. PRI was calculated as $(R_{531} - R_{570})/(R_{531} + R_{570})$, where R_n is the reflectance of the leaf at n nm (Peñuelas et al., 1995).

3.2.3 CO_2 and BVOC exchange measurements

Foliar CO2 and H2O exchanges were measured with the LCpro+ Photosynthesis System (ADC BioScientific). LUE was here calculated as the ratio between the net photosynthetic rates and incident PAR. In order to determine and quantify BVOC exchange, flow meter were used to monitor the air exiting the leaf chamber, which was then analysed using proton transfer reaction–mass spectrometry (PTR–MS; Ionicon Analytik, Innsbruck, Austria). At alternative intervals, the output air flowing from the leaf chamber was also sampled using stainless steel tubes filled with terpene adsorbents, and thereafter analysed by thermal desorption and gas chromatography–mass spectrometry (GC–MS). The difference between the concentration of isoprenoids passing through the chamber clamped to a leaf and the chamber with no leaf, together with the flow rates, were used to calculate the foliar isoprenoid exchange. The tubing used to connect the leaf chamber with the PTR–MS system (50 cm long and 2 mm internal diameter) was made of Teflon. The system used was always the same for all measurements.

3.2.4 The PTR–MS technique

PTR–MS is based on chemical ionization, specifically non-dissociative proton transfer from H_3O^+ ions to most of the common BVOCs, and has been fully described elsewhere (Lindinger et al., 1998). In our experiment, the PTR–MS drift tube was operated at 2.1 mbar and 50 °C, with an E/N (electric field/molecule number density) of around 130 Td (townsend) (1 Td = 10^{-17} V cm^2). The primary ion signal (H_3O^+) was maintained at approximately 6 x 10^6 counts per second. The instrument was calibrated using an aromatic mix standard gas (TO-14A, Restek, Bellefonte, PA, USA) and isoprene and monoterpene standard gas (Abello Linde SA, Barcelona).

3.2.5 Terpene sampling and analysis by GC–MS

Exhaust air from the chambers was pumped through a stainless steel tube (8 cm long and 0.3 cm internal diameter), filled manually with the terpene adsorbents Carbopack B, Carboxen 1,003 and Carbopack Y (Supelco, Bellefonte, Pennsylvania), and separated by plugs of quartz wool. Samples were taken using a Qmax air sampling pump (Supelco, Bellefonte, PE, USA). For more details see Peñuelas et al. 2005. The sampling time was 10 min, and the flow varied between 470 and 500 ml min^{-1} depending on the glass tube adsorbent and quartz wool packing. Glass tubes were stored at -28 °C until the analysis.

Terpene analyses were performed using a GC–MS system (Hewlett Packard HP59822B, Palo Alto, CA, USA). The monoterpenes trapped on the tubes were processed with an automatic sample processor (Combi PAL, FOCUS-ATAS GL International BV 5500 AA Veldhoven, The Netherlands) and desorbed, using an OPTIC3 injector (ATAS GL International BV 5500 AA Veldhoven, The Netherlands), into a 30 x 0.25 x 0.25 mm film capillary column (SPB TM-5 Fused Silica Capillary column; Supelco, Bellefonte, PE, USA). The injector temperature (60 °C) was increased at 16 °C s^{-1} to 300 °C. The injected sample was cryofocused at -20 °C for 2 min. After this time, the cryotrap was heated rapidly to 250 °C. Helium flow was 0.7 ml min^{-1}. Total run time was 23 min and the solvent delay was 4 min. After the sample injection, the initial temperature (40 °C) was increased at 30 °C min^{-1} up to 60 °C, and thereafter at 10 °C min^{-1} up to 150 °C. This temperature was maintained for 3min, and thereafter increased at 70 °C min^{-1} up to 250 °C, and maintained at this temperature for another 5 min. Helium flow was 1 ml min^{-1}.

Monoterpenes were identified by comparing the retention times with standards from Fluka (Buchs, Switzerland), and the fractionation mass spectra with standards, spectra derived from the literature and the GCD Chemstation G1074A HP and the mass spectra library wiley7n. Terpene concentrations were determined from calibration curves. The calibration curves for common monoterpenes, a-pinene, D^3-carene, b-pinene, b-myrcene, *p*-cymene, limonene and sabinene, and common sesquiterpenes such as a-humulene, were determined once every five analyses using four different terpene concentrations. The calibration curves were always highly significant ($r^2 > 99$ for the relationships between the signal and terpene concentrations).

3.2.6 Data treatment

Linear and non-linear curves were fitted using Sigmaplot and statistical tests with Statistica 6.0 software (StatSoft, Tulsa, OK, USA). We used R (RKWard Version 0.6.1) (R Core Team , 2012) to develop empirical models based on the exponential and linear relationships between emissions and PRI found as a result of repeated random sub-sampling of two out of three replicates for each growth condition as the training set for estimating the isoprenoid emission rates. The estimated values were then tested against the values of the remaining randomly selected third set of replicates. This procedure was repeated 1,000 times. Emissions were also estimated with MEGAN model algorithms (Guenter et al., 2006), and with empirical models using MEGAN algorithms complemented with PRI.

3.3 Results

3.3.1 Relationships of isoprenoid emissions with LUE

Isoprenoid emissions were always negatively related to LUE both for isoprene in *P. nigra* and for monoterpenes in *Q. ilex* in response to irradianceand in each environment of drought, senescence and lightgrowth (Fig. 3.1). Under each experimental condition and forindividual leaves, LUE accounted for up to 90% of the variance in isoprene and monoterpene emissions. LUE explained 73 and 72% of the total variance in isoprene and monoterpene emission rates expressed as a percentage of the maximum emission rate measured per plant and growth condition, when the whole data set for all cases and conditions was considered (Fig. 3.2). LUE explained 40 and 42% of the total variance when absolute values of isoprene and monoterpene emission rates were considered (Fig. 3.3). All these relationships still held when considering only the light-saturated conditions with constant net photosynthetic rates and changing electron transport rates (above 250 μmol m^{-2} s^{-1}, Fig. 3.2, Fig. 3.4).

3.3.2 Relationships of isoprenoid emissions with PRI

When we tested PRI thereafter, with the reflectance index used as a proxy for LUE in order to assess isoprene and monoterpene emission rates remotely, we found that, in effect, isoprenoid emissions were negatively related to PRI both for isoprene in *P. nigra* and for monoterpenes in *Q. ilex* in response to irradiance and to each particular drought, senescence and light growth environment (Fig. 3.5). PRI explained more than 90% of the variance in isoprene and monoterpene emission rates for most growth conditions and plants when considered separately and in sunny conditions (Fig. 3.5), and 65% of the variance in isoprene emission rates and 57% of the variance in monoterpene emission rates when considering the whole set of data under all the different drought, light, senescence and sun–shade conditions (Fig. 3.6). It still explained 58 and 47% of the respective variances in isoprene and monoterpene emission rates, respectively, when considering only the light-saturated conditions (above 250 μmol m^{-2} s^{-1}, Fig. 3.6).

We randomly selected two out of the three replicates for each growth condition and used them as the training set for estimating isoprenoid emission rates from PRI. The estimated values were then tested against the values of the remaining randomly selected third set of replicates. This procedure was repeated 1,000 times. We determined there to be a strong fit of the observed emission rates compared with those predicted by the PRI empirical model (RMSE of 2.69 nmol m^{-2} s^{-1} for isoprene emissions and 1.54 nmol m^{-2} s^{-1} for monoterpene emissions; Fig. 3.7).

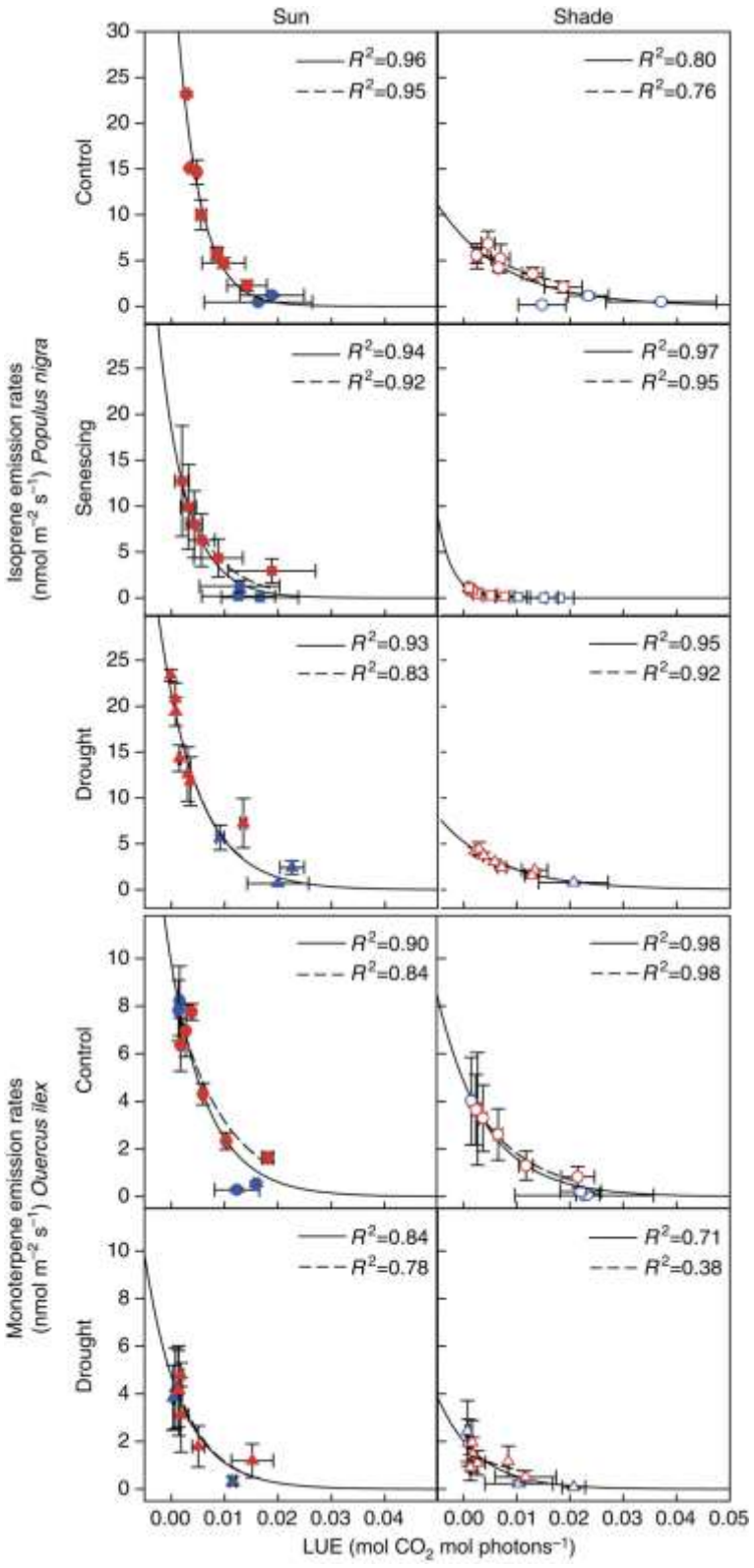

Fig. 3.1: Relationships between foliar isoprenoid emissions and LUE for each growing condition. Isoprene emission rates of *Populus nigr*a and monoterpene emission rates of *Quercus ilex* as a function of light use efficiency (LUE) in control, foliar senescing and droughted plants grown in sunny (closed symbols) and shaded (open symbols) conditions. The red symbols and the dashed lines represent light-saturated conditions for photosynthesis (PAR above 250 µmol m^{-2} s^{-1}). The blue symbols represent values for PAR below 250 µmol m^{-2} s^{-1}, that is, with not saturated photosynthetic rates (Fig. 3.4). The continuous line represents the whole data set. The error bars are ± SE (n=3 plants).

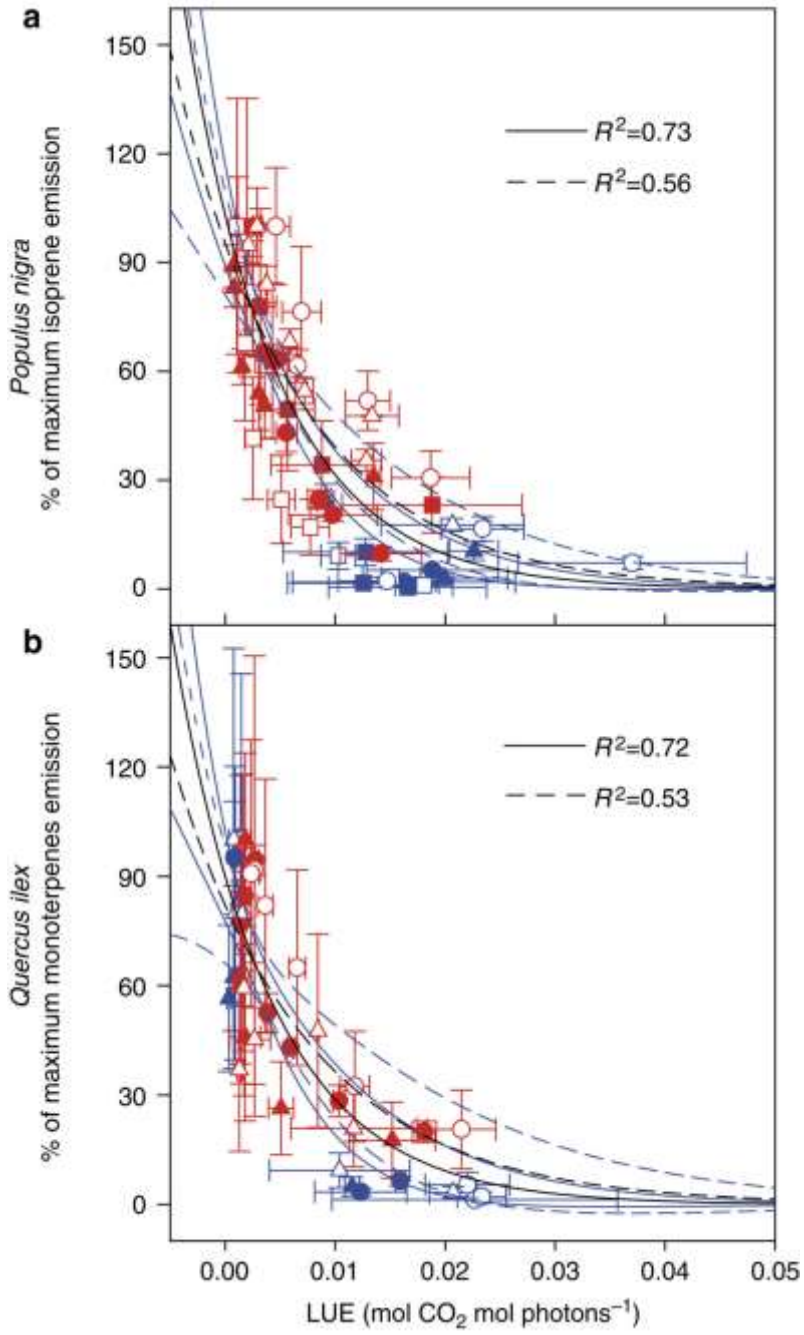

Fig. 3.2: Relationship between isoprenoid emissions and LUE for all growing conditions. Isoprene emission rates of *Populus nigra* (a) and monoterpene emission rates of *Quercus ilex* (b) (relative to the maximum for each plant) as a function of light use efficiency (LUE) considering control, foliar senescing and droughted plants grown in sunny (closed symbols) and shaded (open symbols) conditions altogether. The red symbols and the dashed black line represent light-saturated conditions for photosynthesis (PAR above 250 μmol m^{-2} s^{-1}). The blue symbols represent values for PAR below 250 μmol m^{-2} s^{-1}, that is, with not saturated photosynthetic rates (Fig. 3.4). The continuous black line represents the whole data set. The error bars of the symbols are ± SE (n = 3 plants). SEE, standard error of estimate. 95% Confidence intervals are plotted for both relationships (continuous blue lines for whole data set and dashed blue lines for light-saturated conditions for photosynthesis). For the whole data set: $y=a$ exp ($-bx$) where a=103±7, b=119±15, SEE 17. For the data set on light-saturated conditions: $y=a$ exp ($-bx$) where a=95±7, b=89±16, SEE 18. For the whole data set on monoterpene emissions: $y=a$ exp ($-bx$) where a =90±6, b=114±21, SEE 18. For the data set on light-saturated conditions: $y=a$ exp ($-bx$) where a=82±8, b=81±23, SEE 18.5.

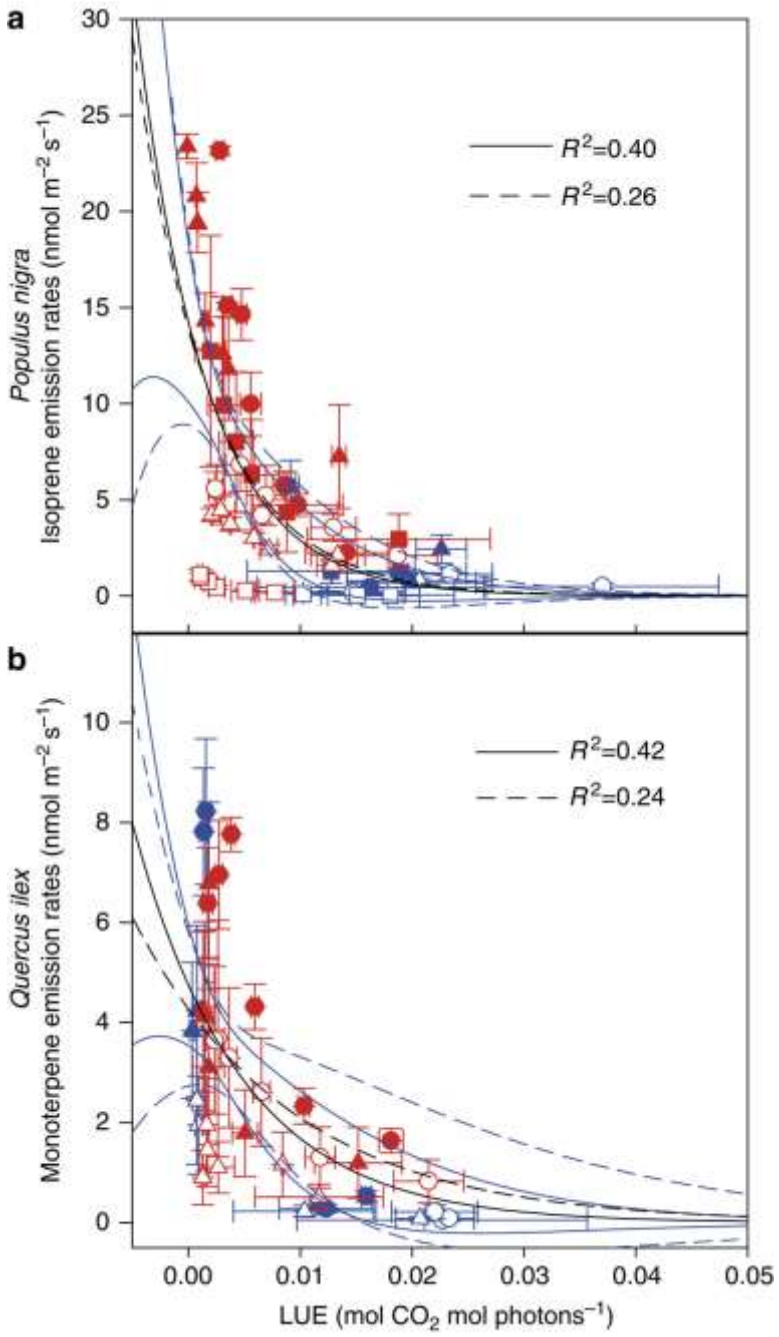

Fig. 3.3: Relationship between isoprenoid emissions and LUE for all growing conditions. Isoprene emission rates of *Populus nigra* (a) and monoterpene emission rates of *Quercus ilex* (b) (expressed in absolute values) as a function of light use efficiency (LUE) considering control, foliar senescing and droughted plants grown in sunny (closed symbols) and shaded (open symbols) conditions altogether. The red symbols and the dashed black line represent light-saturated conditions for photosynthesis (PAR above 250 μmol m^{-2} s^{-1}). The blue symbols represent values for PAR below 250 μmol m^{-2} s^{-1}, that is, with not saturated photosynthetic rates (Fig. 3.4). The continuous black line represents the whole data set. The error bars of the symbols are±s.e. (n=3 plants). SEE, standard error of estimate. 95% Confidence intervals are plotted for both relationships (continuous blue lines for whole data set and dashed blue lines for light-saturated conditions for photosynthesis). For the whole data set: $y=a$ exp ($-bx$) where a=14±2, b=160±41, SEE 4.8. For the data set on light-saturated conditions: $y=a$ exp ($-bx$) where a=14±2.5, b=148±52, SEE 5.6. For the whole data set on monoterpene emissions: $y=a$ exp ($-bx$) where a=4.75±0.6, b=104±35, SEE 1.8. For the data set on light-saturated conditions: $y=a$ exp ($-bx$) where a=4.3±0.7, b=71±38, SEE 1.8.

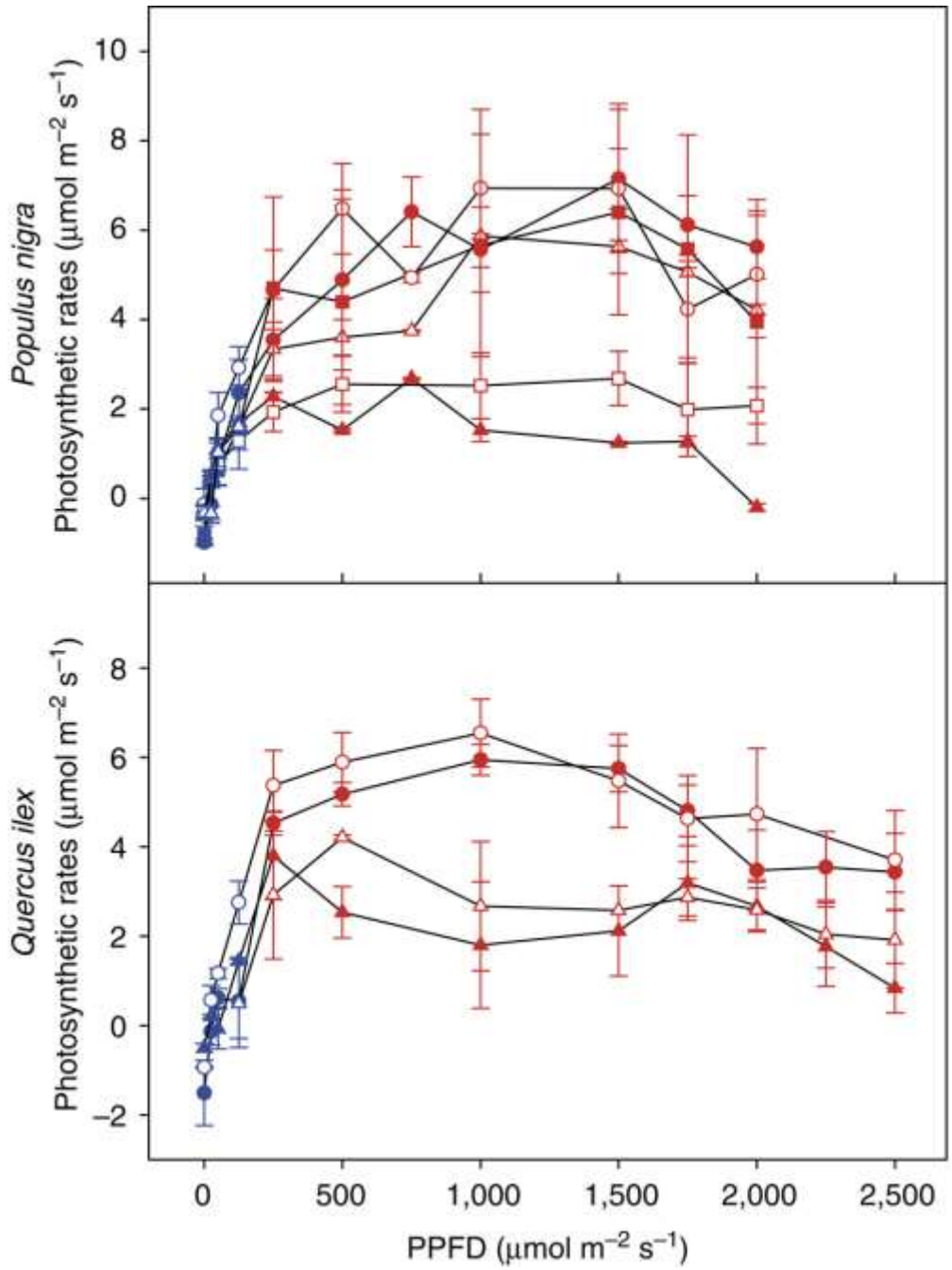

Figure 3.4: Light-response curves of net photosynthetic rates of *Populus nigra* and *Quercus ilex.* Data shown for net photosynthetic rates in control (circles), foliar senescing (squares) and droughted (triangles) plants grown in sunny (closed symbols) and shaded conditions (open symbols). The error bars are ± SE. (n=3 plants). PPFD, photosynthetic photon flux density. The figure shows saturation of net photosynthetic rates at PPFDs above 250 µmol m^{-2} s^{-1} The red symbols represent light-saturated conditions for photosynthesis (PAR above 250 µmol m^{-2} s^{-1}). The blue symbols represent values for PAR below 250 µmol m^{-2} s^{-1}, that is, with non-saturated photosynthetic rates.

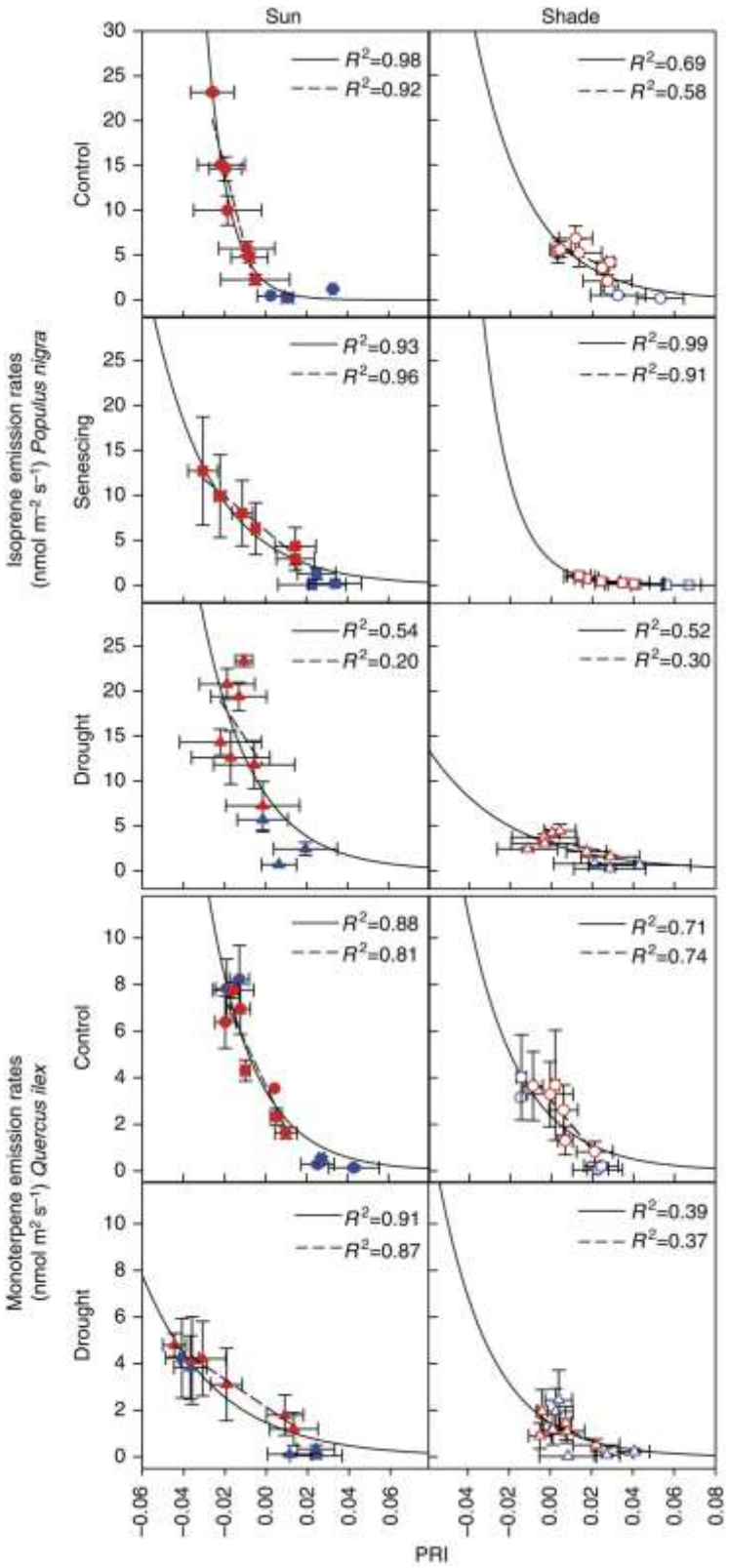

Figure 3.5: The relationships between foliar isoprenoid emissions and PRI for each growing condition. Isoprene emission rates of *Populus nigra* and monoterpene emission rates of *Quercus ilex* as a function of photochemical reflectance index (PRI) in control, foliar senescing and droughted plants grown in sunny (closed symbols) and shaded (open symbols) conditions. The red symbols and the dashed lines represent light-saturated conditions for photosynthesis (PAR above 250 μmol m^{-2} s^{-1}). The blue symbols represent values for PAR below 250 μmol m^{-2} s^{-1}, that is, with not saturated photosynthetic rates (Fig. 3.4). The continuous lines represent the whole data set. The error bars are ± SE (n=3 plants).

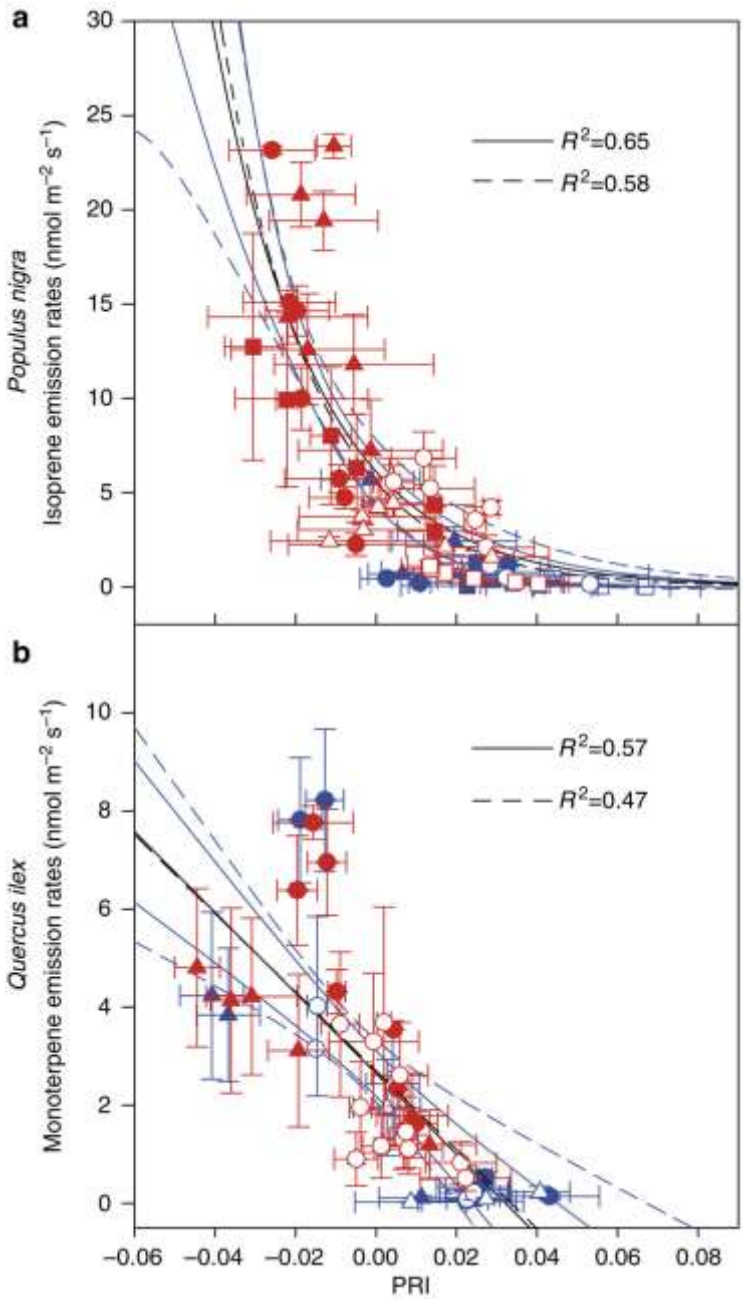

Figure 3.6: Relationship between foliar isoprenoid emissions and PRI for all growing conditions. Isoprene emission rates of *Populus nigra* (a) and monoterpene emission rates of *Quercus ilex* (b) as a function of photochemical reflectance index (PRI) considering control, foliar senescing and droughted plants grown in sunny (closed symbols) and shaded (open symbols) conditions altogether. The red symbols and the dashed black line represent light-saturated conditions for photosynthesis (PAR above 250 μmol m^{-2} s^{-1}). The blue symbols represent values for PAR below 250 μmol m^{-2} s^{-1}, that is, with not saturated photosynthetic rates (Fig 3.4). The continuous black line represents the whole data set. The error bars of the symbols are ± SE (n=3 plants). SEE, standard error of estimate. 95% Confidence intervals are plotted for both relationships (continuous blue lines for whole data set and dashed blue lines for light-saturated conditions for photosynthesis). For the whole data set on isoprene emissions: $y=a$ exp ($-bx$) where a=5.5±0.6, b=43.6±5.6, SEE 3.6. For the data set on light-saturated conditions: $y=a$ exp ($-bx$) where a=6.1±0.8, b=39±7, SEE 4.2. For the whole data set on monoterpene emissions: $y=a$ exp ($-bx$) where a=2.6±0.2, b=−82±11, SEE 1.5. For the data set on light-saturated conditions: $y=a$ exp ($-bx$) where a=2.7±0.3, b=−80±18, SEE 1.5.

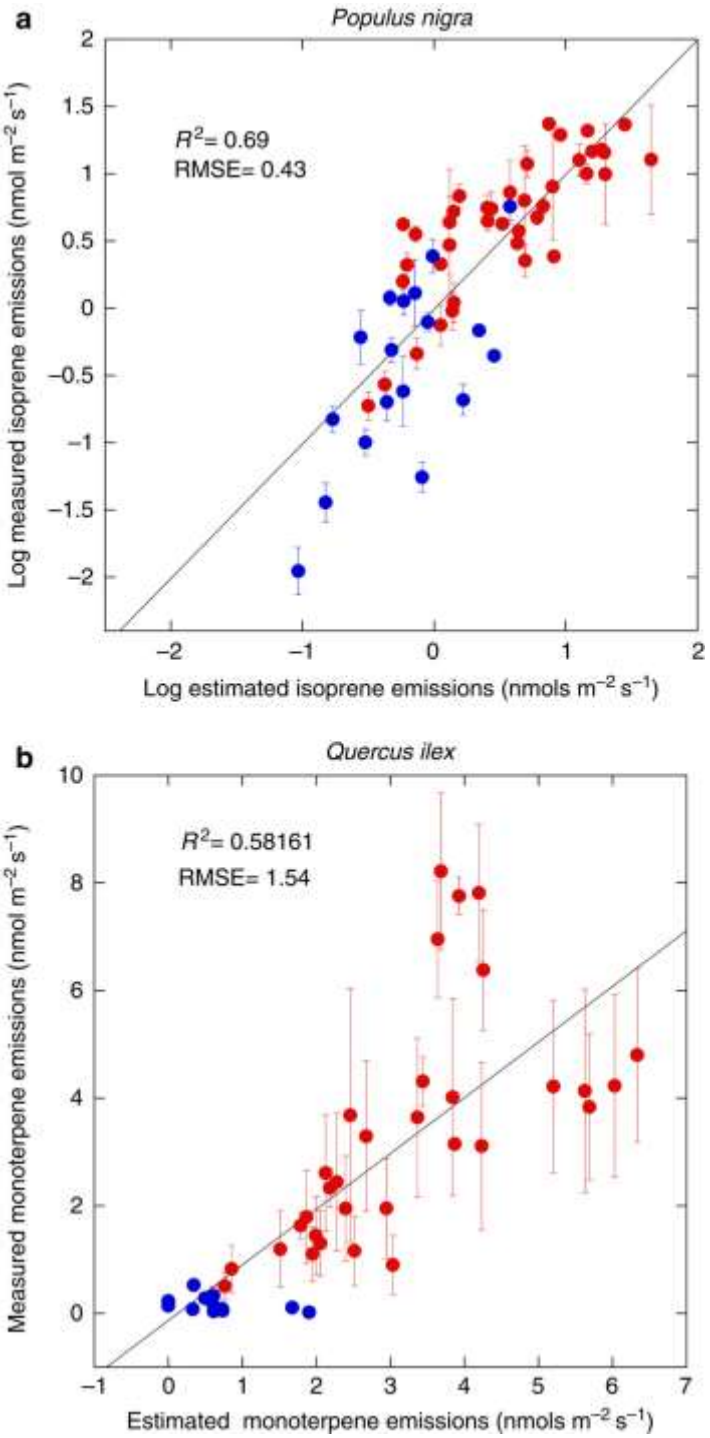

Figure 3.7: Observed versus predicted isoprenoid emission rates. Empirical relationships with PRI are used to plot observed and predicted isoprenoid emission rates on log (a) and normal (b) scales. The error bars are ± SE (n=3 plants). The plotted line is the 1:1 line. The red symbols correspond to light-saturated conditions for photosynthesis (PAR above 250 μmol m^{-2} s^{-1}). The blue symbols represent values for PAR below 250 μmol m^{-2} s^{-1}, that is, with not saturated photosynthetic rates (Fig 3.4).

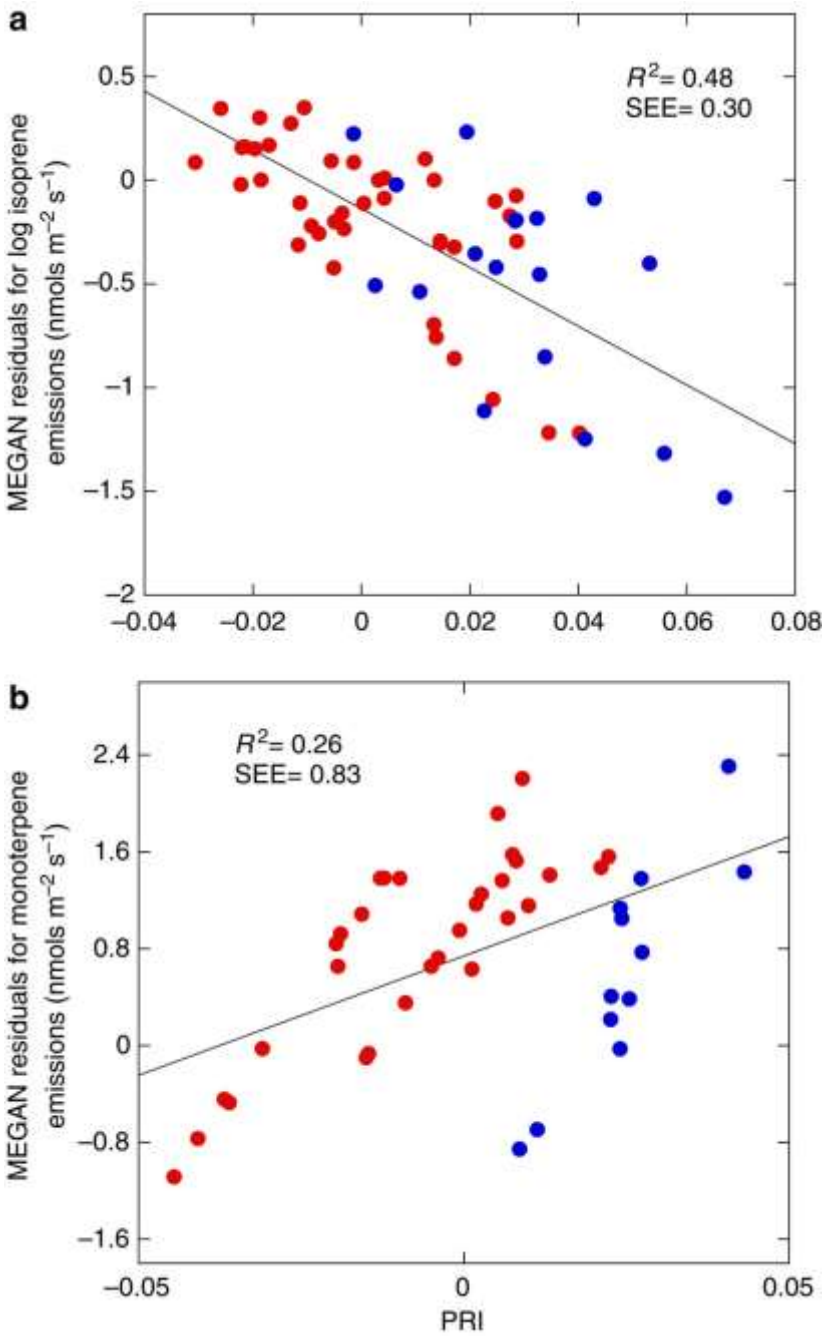

Figure 3.8: Relationships of the residuals of MEGAN-estimated emissions with PRI. Emission rates were expressed as log nmol m^{-2} s^{-1} for isoprene, and as nmol m^{-2} s^{-1} for monoterpenes. No error bars for observations are plotted here; they are shown in Fig. 3.7. The plotted line is the 1:1 line. The red symbols correspond to light-saturated conditions for photosynthesis (PAR above 250 µmol m^{-2} s^{-1}). The blue symbols represent values for PAR below 250 µmol m^{-2} s^{-1}, that is, with not saturated photosynthetic rates (Fig 3.4).

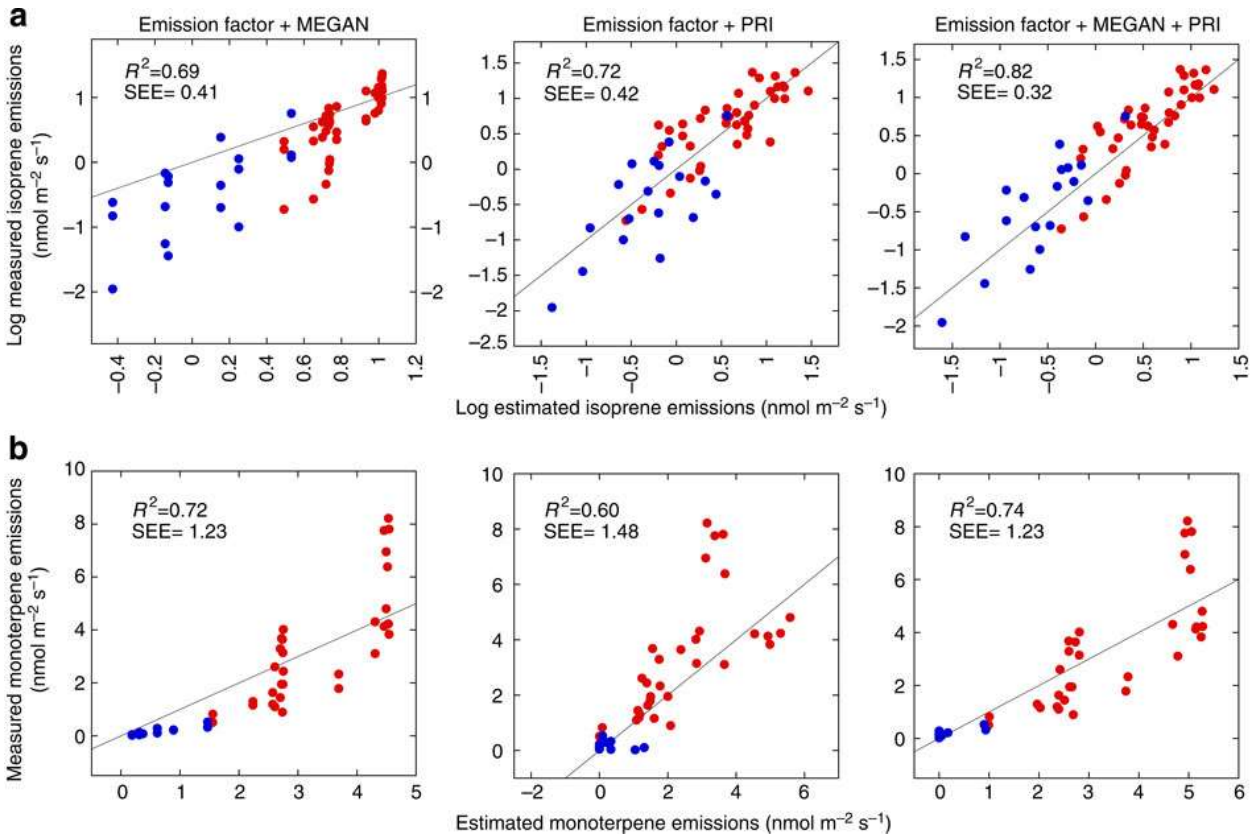

Figure 3.9: Adding PRI to the estimation of isoprenoid emissions. Measured versus estimated isoprenoid emissions using MEGAN model, PRI and MEGAN+PRI to scale the basal emission factors. The plotted line is the 1:1 line. The red symbols correspond to light-saturated conditions for photosynthesis (PAR above 250 µmol m^{-2} s^{-1}). The blue symbols represent values for PAR below 250 µmol m^{-2} s^{-1}, i.e., with not saturated photosynthetic rates (Fig 3.4).

We also found that PRI explained significant variance of theresiduals of the estimations of standard emission models such as MEGAN (Guenter et al., 2006) both for isoprene and monoterpene emissions (Fig. 3.8), and that PRI, together with basal emission factors, was a similar predictor for isoprenoids as these standard emission models (Fig. 3.9). Finally, better predictions for isoprene emissions and similar or slightly better predictions for monoterpene emissions were obtained by complementing MEGAN algorithms with PRI (Fig. 3.9).

3.4 Discussion

The inverse relationships found between isoprenoid emissions and PRI, and therefore the significant predictive value of the latter (RMSE was 2.69 nmol m^{-2} $s^{-1}$for the estimation of emission rates of isoprene ranging from 0 and 25 nmol m^{-2} s^{-1} in *P. nigra* and 1.54 nmol m^{-2} s^{-1} for the estimation of the emission rates of monoterpenes ranging from 0 to 10 µmol m^{-2} s^{-} in *Q. ilex*; Fig. 3.5), fitted well with our hypothesis that isoprenoid emissions could be remotely sensed

using PRI at the leaf level. This remote sensing capacity is based on the relationships that exist between isoprenoid emissions and LUE as a result of the greater availability of photosynthetic reducing power for isoprenoid production under lower LUEs, that is under a higher excess of photosynthetically active radiation (PAR) that is not used for fixing carbon (Morfopoulus et al., in press; Peñuelas & Llusia, 2004; Owen & Peñuelas, 2005) and based on the fact that PRI is already widely tested as a good estimator of LUE at the leaf, canopy and ecosystem levels (Gamon et al., 1992; Peñuelas et al., 2011; Filella et al., 1996; Garbulsky et al., 2011). The better fit of LUE with percentages of isoprenoid emissions relative to the maximum than with absolute values (Figs 3.2, 3.3) warrants further efforts to develop the standardization of the signal for different species, ecosystems and conditions by gaining the necessary knowledge on the scaling physiological and structural processes involved. PRI is a remote sensing index that not only relates to the physiological modulation of the maximum emission rates but also provides assessment of the physiological and structural conditions themselves, thus providing a better fit of absolute emission rates with PRI (Fig. 3.6) than for emissions relative to the maximum (data not shown). LUE

PRI accounted for part of the discrepancy between observed and model-estimated emissions both for isoprene and for monoterpenes (Figs 3.7, 3.8), thus supporting the potential for remote sensing to scale isoprenoid emissions. Because of that, the complementation of MEGAN estimations with PRI improved the predictions of the isoprenoid emissions (Fig. 3.9). The significant part of the variation in emission rates captured by PRI is likely linked to the shifts in basal rates induced by different stress conditions (Niinemets et al., 2010).

PRI was defined at the leaf and canopy levels in the early 1990s in order to assess the efficiency of the use of absorbed photosynthetic active radiation by plants to photosynthesize (LUE) (Gamon et al., 1992; Peñuelas et al., 1995). PRI calculated from the data provided by satellite imaging spectrometers is currently increasingly being applied at the ecosystem level (Garbulsky et al., 2008, 2011; Rahman et al., 2004; Drolet et al. 2008; Xie et al., 2009; Coops et al., 2010; Goerner et al., 2009, 2010; Hilker et al., 2010), opening up the possibility of significantly improving the accuracy of estimating spatial and temporal gross CO_2 uptake by vegetation using remote sensing (Peñuelas et al., 2011; Garbulsky et al., 2011). Now, however, these results also create the possibility of using remote sensing to estimate isoprenoid emissions directly, based on a rough general relationship or at least indirectly through the improved modulation of the estimated emissions from factors of emission capacity (E_c) using PRI. A comparison of the remote sensing of formaldehyde and PRI could validate this approach. PRI could thus substitute the serial empirical functions currently established in the emission models to better estimate current emissions. A complementary use of the remote sensing of

formaldehyde and PRI could validate this approach. Adding information from PRI to the emission models might at least help to capture some spatial and temporal variability that the current models presently miss.

PRI was originally defined to assess the short-term xanthophyll pigment changes that accompany plant stress (Gamon et al., 1990; Peñuelas et al., 1994). These changes are linked to the dissipation of the excess absorbed energy that cannot be processed through photosynthesis, and which therefore reduces LUE 38. This excess absorbed energy is available for isoprenoid production (Morfopoulus et al., in press; Peñuelas & Llusia, 2004; Owen & Peñuelas, 2005). As these pigment changes translate into changes in reflectance at 531 nm, and as a reflectance of 570nm is instead insensitive to short-term changes in these pigments, the PRI was defined as $(R_{531} - R_{570})/(R_{531} + R_{570})$, where R indicates reflectance and numbers indicate wavelength in nanometers (Gamon et al., 1992; Peñuelas et al., 1995). Furthermore, the relationship with LUE is reinforced by the fact that PRI also measures the relative reflectance on either side of the green reflectance 'hump' (550 nm), that is, the reflectance in the blue region (chlorophyll and carotenoid absorption) of the spectrum relative to the reflectance in the red region (chlorophyll absorption only). Consequently, it also behaves as an index of chlorophyll: carotenoid ratios and therefore of the photosynthetic activities associated with their changes during leaf development, aging or stress in the longer term (Peñuelas et al., 1997; Sims & Gamon, 2002; Filella et al. 2009); it will probably also present an inverse relationship with isoprenoid emissions, as isoprenoids are also linked with carotenoids (Owen et al., in press).

The isoprenoid–PRI relationships described here fit our current understanding of the physiological processes involved in isoprenoid emissions. Our study shows the potential of this PRI technique to validate the availability of photosynthetic reducing power as a factor involved in isoprenoid production and fits our hypothesis of isoprenoid emissions correlating with other more efficient energy quenching processes such as the xanthophyll cycle. Isoprenes and monoterpenes are synthesized via the plastidic 2-*C*-methyl-D-erythritol 4-phosphate pathway (Lichtenthaler et al., 1999), which is also the beginning of the synthesis route for essential metabolites, including the photoprotective compounds (carotenoids, tocopherol)43 produced under stress conditions and lower LUE values. Demand for the various downstream products of the 2-*C*-methyl-D-erythritol 4-phosphate pathway can be a significant drain on photoassimilates, energy supply and reducing power (Owen & Peñuelas, 2005; Loreto & Sharkey, 1993; Li & Sharkey, 2013). The isoprenoid synthesis pathway consumes large amounts of photosynthetically formed adenosine triphosphate (ATP) and nicotinamide adenine dinucleotide phosphate (NADPH), and may thus serve as a 'safety valve' that is useful in avoiding over-reduction and photoinhibition of the photosynthetic apparatus (Morfopoulus et al., in press;

Peñuelas & Llusia, 2004; Owen & Peñuelas, 2005; Lichtenthaler, 2007). In fact, trade-offs between the attainment of optimal photosynthetic rates and volatile isoprenoids would appear to be inevitable when considering the overall allocation of carbon and energy supplies (Morfopoulus et al., in press; Peñuelas & Llusia, 2004; Owen & Peñuelas, 2005). Isoprene and monoterpene emissions should thus be negatively correlated with LUE and with PRI. This is what we found here. Our results tend to confirm this hypothesis. PRI was negatively correlated with isoprenoid emissions that increased with rising irradiance and decreasing LUE. PRI was also effective in assessing isoprenoid emissions in senescing leaves but not in leaves of saplings suffering from drought conditions. This drought-related disturbance in the LUE–PRI relationship has already been found in the first studies using PRI to assess LUE under drought stress (Gamon et al., 1990, 1992).

Isoprenoid emissions were negatively related to changes in LUE, both for isoprene in *P. nigra* and for monoterpenes in *Q. ilex* in response to irradiance, in each particular light growth environment (Fig. 3.1). ATP and NADPH are needed in order to produce dimethylallyl diphosphate (DMAPP), the synthesis precursor of isoprene and monoterpenes (Rasulov et al., 2011). There are more 'excess' electrons (and carbon chains) available for isoprene production in high than in low irradiance. Plants grown in full sunlight moreover develop higher capacities for the synthesis of isoprene and monoterpenes than do plants grown in the shade (Fig. 3.1). When photosynthesis is electron transport-limited (in low light conditions), the shortfall of ATP and NADPH for CO_2 assimilation may cause a deficit in the reducing power available to transform carbohydrates into DMAPP. When photosynthesis is Rubisco-limited (in full light conditions), the plant may use a proportion of the ATP and NADPH excess (resulting from an excess of electrons produced by photochemical reactions) to reduce carbohydrates to DMAPP (Morfopoulus et al., in press; Peñuelas & Llusia, 2004; Owen & Peñuelas, 2005; Rasulov et al., 2011) and, as a result, isoprenoid emissions increase when light availability exceeds photosynthetic capacity. The fraction of the assimilated carbon allocated to isoprene production increases with increasing light intensity, even when photosynthesis is light-saturated (Sharkey & Loreto, 1993).

Senescent leaves had slightly lower emission rates in our study and strong relationships with both LUE and PRI. The literature regarding isoprenoid emissions in ageing leaves is not very consistent: some studies suggest that the biochemical capacity to produce isoprene is unaffected by senescence, some others suggest that isoprene declines before photosynthesis, whereas some argue that measurable isoprene emission persists in senescing leaves even after the cessation of photosynthesis (Morfopoulus et al., in press). In poplars grown under conditions of elevated CO_2, isoprene emission was sustained for longer periods in senescing leaves, whereas

the decline in photosynthesis was accelerated (Centritto et al., 2004). Under these conditions, Tallis et al. (2010) demonstrate an increased expression of genes involved in glycolysis, suggesting that phosphoenolpyruvic acid from glycolysis, translocated to the chloroplast, may provide the substrate for sustained isoprenoid emission in senescing leaves (Loreto et al., 2007).

Under drought conditions, C_i (internal CO_2) is reduced, as is photosynthetic carbon fixation (Fig. 3.4) Although isoprenoid emissions are dependent on photosynthesis for the supply of energy (ATP), reducing power (NADPH) and carbon skeletons, several environmental and ontogenetic factors decouple the two processes. For instance, soil water deficits reduce photosynthetic carbon assimilation, whereas isoprene emissions can continue at a high level (Loreto et al., 2007). Light-dependent isoprene emission has been observed in leaves that have been severed at the stem and have ceased to photosynthesize (Loreto & Schnitzler, 2010; Brilli et al. 2011).

At the leaf and canopy levels, there is an emerging consistency in the LUE–PRI relationship that suggests a functional convergence of biochemical, physiological and structural components affecting leaf, canopy and ecosystem carbon uptake efficiencies. The use of PRI as a proxy of LUE has extended exponentially in the last few years, both in natural and seminatural vegetation and in crops (Garbulsky et al., 2011). The results of these studies confirm an exponential relationship between LUE and PRI over a wide range of species
and conditions, therefore suggesting that the relationship of isoprenoid emissions with PRI may also hold well when upscaled to the canopy and ecosystem scales. The high spectral resolution sensors on satellite platforms, such as the moderate resolution imaging spectroradiometer MODIS sensor on the TERRA and AQUA satellites, might therefore be used for global assessment of isoprenoid emissions.

The results showed that the different sapling treatments with different environmental constraints and different LUE values present a different parameterization of their isoprenoid–PRI relationships, as happens with LUE–PRI exponential relationships (Garbulsky et al., 2011; Goerner et al., 2010).

PRI can be improved in the near future with standardization by species or biomes or environmental conditions, for example by comparison with different sensor angles or using other approaches in order to buffer the disturbing effects of geometry and structure of each type of species or ecosystem or environmental condition. However, in any case, although only approximate, there was a common exponential relationship between isoprenoid emissions and PRI, as there was for LUE–PRI relationships (Garbulsky et al., 2011) (Figs 3.2, 3.4). Furthermore, even if no general isoprenoid emissions–PRI relationship can finally be established, PRI could at least be used as a modulator or scaling factor for the basal emission

factors used for each species, biome or set of conditions (Figs 3.1, 3.5, 3.9). The species- and ecosystem-specificity of BVOC emissions–PRI response curves creates a similar restriction to that of the current approach of using basal emission rates, but the use of PRI introduces a key improvement because PRI assesses emission rates actually, instead of assuming constant basal emission factors that in fact are very variable (Niinemets et al., 2010). Satellite sensors such as MODIS can make suitable reflectivity measurements only once a day at a given location on the Earth in cloud free conditions. The PRI would thus suffer from an inherent clear sky bias, but it could be complemented with the use of remote sensing signals for HCHO that contain the underlying signature of BVOC emitted in both cloudy and clear sky conditions.

These results therefore provide a challenging and exciting new way of potentially assessing isoprenoid emissions from terrestrial ecosystems, something which is essential for a more accurate quantification of global isoprenoid emissions and an understanding of their variability. PRI, as a proxy of isoprenoid emissions and LUE, can be used to complement the normalized difference vegetation index or other indices such as enhanced vegetation index, which are proxies of green biomass-fraction of absorbed PAR, in order to estimate canopy isoprenoid emission rates.

There are other steps to take up before the generalization of PRI from the leaf level to the ecosystem and biospheric scales, and its global and operational use as an estimator of isoprenoid emissions. In brief, similar issues as those for PRI assessment of LUE at the ecosystem and biospheric scales can be encountered. These issues can be related to structural differences in the canopies, to varying ‘background effects’ (for example, soil colour, moisture, shadows, or the presence of other non-green landscape components), or to the different reflectance signals derived from illumination and variations in viewing angles (Hilker et al., 2010; Filella et al., 2004; Sims et al. 2006). Because of these issues, PRI may be more broadly applicable and portable across climatically and structurally different biome types when the differences in canopy structure are known (Hilker et al., 2010). However, several studies have found an emerging consistency in the relationship between PRI, LUE and ecosystem CO2 uptake (Garbulsky et al., 2008, 2011; Rahman et al., 2004; Drolet et al. 2008; Goerner et al., 2009, 2010; Xie et al., 2009; Coops et al., 2010), suggesting a surprising degree of ‘functional convergence’ in the biochemical, physiological and structural components affecting ecosystem carbon fluxes (Field, 1991), which can now be extended to isoprenoid emissions. In other words, ecosystem functioning possesses emergent properties that may allow us to explore their seemingly complex isoprenoid and photosynthetic behavior effectively by using surprisingly simple optical sampling methods, such as the measurement of PRI or other remote sensing indices, algorithms and products that may emerge from the research effort in this area.

Understanding the basis for this convergence and unearthing the 'ecophysiological rules' governing these responses each remain a primary goal of current ecophysiological research. Meanwhile, of importance for the pragmatic empirical remote sensing of isoprenoid emissions, PRI can assess the LUE of ecosystems, in particular from near-nadir satellite observations (Goerner et al. 2010); with multiangle atmospheric correction (Hilker et al., 2010), (Lyapustin, & Wang, 2009) PRI also has the capacity to become an excellent tool in the continuous global monitoring of isoprenoid emissions, something that is essential in determining their chemical and climatic effects. The launching of a new image spectrometer, such as the NASA HyspIRI or the German EnMAP, will allow PRI to be calculated even at 30-m resolution: this offers great potential. The use of PRI will enable a better estimation of isoprenoid emissions, either through direct empirical estimates or through improved modelling, by modulating the emission factors for ecosystems and biomes rather than multiple complicated climatic, historical, and structural factors.

References

Arneth, A., Monson, R. K., Schurgers, G., Niinemets, U., Palmer, P. I., 2008. Why are estimates of global isoprene emissions so similar (and why is this not so for monoterpenes)? Atmos. Chem. Phys. 8, 4605–4620.

Arneth, A. et al., 2010. Terrestrial biogeochemical feedbacks in the climate system.Nat. Geosci. 3, 525–532.

Barkley, M. P. et al., 2008. Net ecosystem fluxes of isoprene over tropical South America inferred from Global Ozone Monitoring Experiment (GOME) observations of HCHO columns. J. Geophys. Res. 113, D20304.

Brilli, F. et al., 2011. Detection of plant volatiles after leaf wounding and darkening by proton transfer reaction 'time-of-flight' mass spectrometry (PTR-TOF). PLoS One 6, e20419.

Carslaw, K. S. et al., 2010. A review of natural aerosol interactions and feedbacks within the Earth system. Atmos. Chem. Phys. 10, 1701–1737.

Centritto, M., Nascetti, P., Petrilli, L., Raschi, A., Loreto, F., 2004. Profiles of isoprene emission and photosynthetic parameters in hybrid poplars exposed to free-air CO2 enrichment. Plant. Cell Environ. 27, 403–412.

Coops, N. C., Hilker, T., Hall, F. G., Nichol, C. J., Drolet, G. G., 2010. Estimation of light-use efficiency of terrestrial ecosystems from space: a status report. BioScience 60, 788–797.

Demmig-Adams, B., 1990. Carotenoids and photoprotection in plants: A role for the xanthophyll zeaxanthin. Biochim. Biophys. Acta 1020, 1–24.

Drolet, G. G. et al., 2008. Regional mapping of gross light-use efficiency using MODIS spectral indices. Remote Sens. Environ. 112, 3064–3078.

Field, C. B. Response of Plants to Multiple stresses. (eds Mooney, H. A., Winner, W. E., Pell, E. J.) 35–65 (Academic Press, San Diego, 1991).

Filella, I., Amaro, T., Araus, J. L., Peñuelas, J., 1996. Relationship between photosinthetic radiation-use efficiency of barley canopies and the photochemical reflectance index (PRI). Physiol. Plant. 96, 211–216.

Filella, I. et al., 2009. PRI assesment of long-term changes in carotenoids/chlorophyll ratio and short-term changes in de-epoxidation state of the xanthophyll cycle. Int. J. Remote Sens. 30, 4443–4455.

Filella, I., Peñelas, J., Llorens, L., Estiarte, M., 2004. Reflectance assessment of seasonal and annual changes in biomass and CO2 uptake of a Mediterranean shrubland submitted to experimental warming and drought. Remote Sens. Environ. 90, 308–318.

Gamon, J., Field, C., Bjorkman, O., Artree, A., Peñuelas, J., 1990. Remote sensing of the xantophyll cycle and chlorophyll fluorescence in sunflower leaves and canopies. Oecologia 85, 1–7.

Gamon, J. A., Peñuelas, J., Field, C. B., 1992. A narrow-waveband spectral index that tracks diurnal changes in photosunthetic efficiency. Remote Sens. Environ. 41, 35–44.

Garbulsky, M. F., Peñuelas, J., Papale, D., Filella, I., 2008. Remote estimation of carbon dioxide uptake by a Mediterranean forest. Global Change Biol. 14, 2860–2867.

Garbulsky, M. F., Peñuelas, J., Gamon, J., Inoue, Y., Filella, I., 2011. The photochemical reflectance index (PRI) and the remote sensing of leaf, canopy and ecosystem radiation use efficiencies. A review and meta-analysis. Remote Sens. Environ. 115, 281–297.

Goerner, A. et al., 2010. Remote sensing of ecosystem light use efficiency with MODIS-based PRI – the DOs and DON'Ts. Biogeosciences Discuss. 7, 6935–6969.

Goerner, A., Reichstein, M., Rambal, S., 2009. Tracking seasonal drought effects on ecosystem light use efficiency with satellite-based PRI in a Mediterranean forest. Remote Sens. Environ. 113, 1101–1111.

Guenther, A. et al., 1995. A global model of natural volatile organic compound emissions. J. Geophys. Res. 100, 8873–8892.

Guenther, A. et al., 2006. Estimates of global terrestrial isoprene emissions using MEGAN (Model of Emissions of Gases and Aerosols from Nature). Atmos. Chem. Phys. 6, 3181–3210.

Hilker, T. et al., 2010. Remote sensing of photosynthetic light-use efficiency across two forested biomes: spatial scaling. Remote Sens. Environ. 114, 2863–2874.

Karl, T., Guenther, A., Spirig, C., Hansel, A., Fall, R., 2003. Seasonal variation of biogenic VOC emissions above a mixed hardwood forest in northern Michigan. Geophys. Res. Lett. 30, 2186.

Kiendler-Scharr, A., Wildt, J., Dal Maso, M., Hohaus, T., Kleist, E., Mentel, T. F., Tillmann, R., Uerlings, R., Schurr, U., and Wahner, A., 2009. New particle formation in forests inhibited by isoprene emissions, Nature, 461, 381–384

Li, Z., Sharkey, T. D., 2013. Metabolic profiling of the methylerythritol phosphate pathway reveals the source of post-illumination isoprene burst from leaves. Plant Cell Environ. 36, 429–437.

Lichtenthaler, H. K., 1999. The 1-deoxy-D-xylulose-5-phosphate pathway of isoprenoid biosynthesis in plants. Annu. Rev. Plant Physiol. Plant Mol. Biol. 50, 47–65.

Lichtenthaler, H. K., 2007. Biosynthesis, accumulation and emission of carotenoids, alpha-tocopherol, plastoquinone, and isoprene in leaves under high photosynthetic irradiance. Photosynth. Res. 92, 163–179.

Lindinger, W., Hansel, A., Jordan, A., 1998. On-line monitoring of volatile organic compounds at pptv levels by means of Proton-Transfer-Reaction Mass Spectrometry (PTR-MS). Medical applications, food control and environmental research. Int. J. Mass Spectrom. Ion Proc. 173, 191–241.

Loreto, F. et al., 2007. The relationship between isoprene emission rate and dark respiration rate in white poplar (Populus alba L.) leaves. Plant Cell Environ. 30, 662–669.

Loreto, F., Schnitzler, J. P., 2010. Abiotic stresses and induced BVOCs. Trends Plant Sci. 15, 154–166.

Loreto, F., Sharkey, T. D., 1993. On the relationship between isoprene emission and photosynthetic metabolites under different environmental conditions. Planta 189, 420–424.

Lyapustin, A., Wang, Y. in Satellite Aerosol Remote Sensing over Land. (eds Kokhanovky, A. & De Leeuw, G.) 69–99 (Springer, 2009).

McKinney, K. A., Lee, B. H., Vasta, A., Pho, T. V. & Munger, J. W., 2011. Emissions of isoprenoids and oxygenated biogenic volatile organic compounds from a New England mixed forest. Atmos. Chem. Phys. 11, 4807–4831.

Misztal, P. K., Karl, T., Guenther, A. B., Jonsson, H. H. & Goldstein, A., 2013. H. PTRMS measurements of eddy covariance fluxes and concentrations of VOCs from aircraft over California. 6th International Conference on Proton Transfer Reaction Mass Spectrometry and its Applications. Conference Series, 125–128 Innsbruck University Press.

Monson, R. K., Grote, R., Niinemets, U. & Schnitzler, J. P., 2012 Modeling the isoprene emission rate from leaves. New Phytol. 195, 541–559.

Morfopoulus, C. et al., in press. A unifying conceptual model for the environmental responses of isoprene emissions from plants. Ann. Bot. doi:10.1093/aob/mct206.

Niinemets, U., 2010. Mild versus severe stress and BVOCs: thresholds, priming and consequences. Trends Plant Sci. 15, 145–153.

Niinemets, U. et al., 2010a. The leaf-level emission factor of volatile isoprenoids: caveats, model algorithms, response shapes and scaling. Biogeosciences 7,1809–1832.

Niinemets, U. et al., 2010b. The emission factor of volatile isoprenoids: stress, acclimation, and developmental responses. Biogeosciences 7, 2203–2223.

Owen, S. M., Peñuelas, J., 2005. Opportunistic emissions of volatile isoprenoids. Trends Plant Sci. 10, 420–426.

Owen, S. M., Peñuelas, J., in press. Volatile isoprenoid emission potentials are correlated with essential isoprenoid concentrations in five plant species. Acta Physiol. Plant doi:10.1007/s11738-013-1344-4.

Pacifico, F., Harrison, S. P., Jones, C. D., Sitch, S., 2009. Isoprene emissions and climate. Atmos. Environ. 43, 6121–6135.

Peñuelas, J., Filella, I., Gamon, J., 1995. Assessment of plant photosynthetic radiation-use efficiency with spectral reflectance. New Phytol. 131, 291–296.

Peñuelas, J., Filella, I., Gamon, J., Field, C. B., 1997. Assessing photosynthetic radiation-use efficciency of emergent aquatic vegetation from spectral reflectance. Aquat. Bot. 58, 307–315.

Peñuelas, J., Gamon, J., Freeden, A., Merino, J., Field, C., 1994. Reflectance indices associated with physiological changes in nitrogen- and water-limited sunflower leaves. Remote Sens. Environ. 48, 135–146.

Peñuelas, J., Garbulsky, M., Filella, I., 2011. Photochemical reflectance index (PRI) and remote sensing of plant CO2 uptake. New Phytol. 191, 596–599.

Peñeulas, J., Llusia, J., 2003. BVOCs: plant defense against climate warming? Trends Plant Sci. 8, 105–109.

Peñuelas, J., Llusia, J., 2004. Plant VOC emissions: making use of the unavoidable. Trends Ecol. Evol. 19, 402-404.

Peñuelas, J., Llusia, J., Asensio, D., Munné-Bosch, S., 2005. Linking isoprene with plant thermotolerance, antioxidants and monoterpene emissions. Plant. Cell. Environ. 28, 278–286.

Peñuelas, J., Munné-Bosch, S., Llusia, J., Filella, I., 2004. Leaf reflectance and photo and antioxidant protection in field-grown summer-stressed Phillyrea angustifolia. Optical signals of oxidative stress? New Phytol. 162, 115–162.

Peñuelas, J., Staudt, M., 2010. BVOCs and global change. Trends Plant Sci. 15, 133–144.

R Core Team., 2012. R: A Language and Environment for Statistical Computing. R Foundation for Statistical Computing 1, 1651.

Rahman, A. F., Cordova, V. D., Gamon, J. A., Schmid, H. P., Sims, D. A., 2004. Potential of MODIS ocean bands for estimating CO2 flux from terrestrial vegetation: A novel approach. Geophys. Res. Lett. 31, L10503.

Rasulov, B., Huve, K., Laisk, A., Niinemets, U., 2011. Induction of a longer term component of isoprene release in darkened aspen leaves: origin and regulation under different environmental conditions. Plant Physiol. 156, 816–831.

Sharkey, T. D., Loreto, F., 1993. Water stress, temperature, and light effects on the capacity for isoprene emission and photosynthesis of kudzu leaves. Oecologia 95, 328–333.

Sims, D.A., Gamon, J. A., 2002. Relationships between leaf pigment content and spectral reflectance across a wide range of species, leaf structures and developmental stages. Remote Sens. Environ. 81, 337–354.

Sims, D.A. et al., 2006. Parallel adjustments in vegetation greenness and ecosystem CO2 exchange in response to drought in a southern California chaparral ecosystem. Remote Sens. Environ. 103, 289–303.

Spirig, C. et al., 2005. Eddy covariance flux measurements of biogenic VOCs during ECHO 2003 using proton transfer reaction mass spectrometry. Atmos. Chem. Phys. 5, 465–481.

Stavrakou, T. et al., 2009. Global emissions of non-methane hydrocarbons deduced from SCIAMACHY formaldehyde columns through 2003-2006. Atmos. Chem. Phys. 9, 3663–3679.

Tallis, M. J. et al., 2010. The transcriptome of Populus in elevated CO2 reveals increased anthocyanin biosynthesis during delayed autumnal senescence. New Phytol. 186, 415–428.

Westberg, H. et al., 2001. Measurement of isoprene fluxes at the PROPHET site. J. Geophys. Res. 106, 24347–24358.

Xie, X., Gao, W., Gao, Z., 2009. Estimating photosynthetic light-use efficiency of Changbai Mountain by using MODIS-derived photochemical reflectance index.Proc. of SPIE 7454, 745415.

CHAPTER 4

Root-to-shoot signaling during drought stress in Populus nigra, an isoprene emitting species.

Giovanni Marino[a,b], Cecilia Brunetti[c], Franco Biasioli[d], Roberto Tognetti[a], Mauro Centritto[b]

[a] Dipartimento di Bioscienze e Territorio, Università degli Studi del Molise, Contrada Fonte Lappone, 86090 Pesche, IS, Italy
[b] Istituto per la Protezione delle Piante, Consiglio Nazionale delle Ricerche, Via Madonna del Piano 10, 50019 Sesto Fiorentino, FI, Italy
[c] Dipartimento di Scienze delle Produzioni Agroambientali e dell'Ambiente, Piazzale delle Cascine, 18, 50144 Firenze, Italy
[d] Centro Ricerca e Innovazione, Fondazione Edmund Mach, Via E. Mach 1, 38010, San Michele all'Adige, TN , Italy

ABSTRACT

A supposed functional role of isoprene emission from leaves is to counter the deleterious effects of excess excitation energy when photosynthesis is severely constrained, for example during drought stress events. Isoprene is produced through the chloroplastic 2-C-methylerythritol-5-phosphate (MEP) pathway which also generate abscisic acid (ABA), that has dominant role in root to shoot singaling under drought stress. On the other hand, in many recent studyes has been observed an antagonistic role between ABA and ethylene in the stomatal regulation in response to water stress conditions. The responses of the isoprene emitting species *Populus nigra* to different water regimes, including partial root zone drying, have been observed to dissect hydraulic and chemical components of root-to-shoot signaling, in order to investigate the potential link between isoprene and ABA biosynthesis, and estimate the interaction effects of ABA and ethylene. Leaf water potential, gas exchanges, chlorophyll fluorescence and volatiles emission have been measurements on plants grown in a split-root system. The partial root zone drying did not affect the hydraulic conditions of plants, leading to a physiological status of partially watered plats that was similar to well watered controls. Results of our study suggest that the hydraulic signal mostly regulated the accumulation of ABA in leaves and did not evidence a clear relation between isoprene and ABA biosynthesis. On the other hand, our study reveals a clear antagonism between ABA and ethylene emission by the leaf during drought stress, indeed the high foliar ABA concentration inhibited the conversion of the ethylene precursor ACC to produce ethylene.

4.1 Introduction

Isoprene (2-methyl-1,3-butadiene) is a volatile organic compound emitted in vast amounts from photosynthesizing leaves of many plant species. Current interest in understanding the environmental and physiological regulation of isoprene formation in plants comes not only from its importance for plant fitness, but also from its implications in atmospheric chemistry (Penuelas & Llusia, 2003). A significant portion of fresh assimilated carbon is invested to isoprene biosynthesis, but plants greatly benefit from isoprene emission when suffering from a wide range of stresses (Vickers et al., 2009). Isoprene scavenges reactive oxygen/nitrogen species (Loreto & Velikova, 2001) and improves the stability of thylakoid membranes (Velikova et al., 2011). These functional roles are of crucial significance in countering the deleterious effects of excess excitation energy when photosynthesis is severely constrained, for example during drought stress events. The reduction of leaf gas exchange is an early response to water limitation, whereas isoprene emission appears to be stimulated under moderate drought stress (Beckett et al., 2012; Tattini et al., 2014). Moreover, isoprene biosynthesis is decoupled from photosynthesis also in plants suffering from severe drought stress (Bruggemann & Schnitzler, 2002; Brilli et al., 2007; Centritto et al., 2011). Indeed, plants invest increasing amount of fresh assimilated carbon for isoprene biosynthesis even when the assimilation of fresh carbon is deeply compromised. Even more, plants may use extra-chloroplastic carbon sources (e.g. breakdown of starch or mitochondrial respiration) for isoprene production when drought-induced stomatal limitations totally inhibit the main source of carbon for isoprene biosynthesis (Affek & Yakir, 2003; Karl et al., 2002; Funk et al., 2004; Wolfertz et al. 2004; Kreuzwieser et al. 2002; Schnitzler et al., 2010).

Isoprene is produced through the chloroplastic 2-C-methylerythritol-5-phosphate (MEP) pathway (Lichtenthaler et al., 1997), which also generate more complex isoprenoids, such as carotenoids and abscisic acid (ABA). ABA plays a pivotal role in drought stress responses, e.g., tightly regulating stomatal opening (Wilkinson & Davies, 2010). An increase in xylem sap ABA concentration has been reported to increase photosynthetic water use efficiency (WUE) during progressive soil drying (Liu et al., 2005a and 2005b). In a wide range of poplars isoprene emission has been also positively correlated with WUE (Guidolotti et al., 2011). The potential relationship between isoprene and ABA has been recently investigated using transgenic tobacco plants under drought stress. Isoprene emitting lines had greater WUE than non-emitting lines. It is possible that during drought stress isoprene emitting species may benefit from a better control of transpirational water loss as compared with non emitting species. In addition, it has been hypothesized that isoprene emission may enhance the flux of carbon in the MEP pathway, thus

leading to an increase in foliar ABA concentration in tobacco leaves during severe stress (Tattini et al., 2014). This results confirms that isoprene may be a proxy of ABA as previously reported from Barta and Loreto (2006).

ABA-mediated stomatal closure may occur through both a direct effect on stomata guard cells (Desikan et al., 2004) and a remote effect by decreasing leaf hydraulic conductance through inactivation of bundle sheath aquaporins (Pantin et al., 2013). A dominant role for ABA in root to shoot singaling under drought stress was demostrated in early reports (Davies & Zhang, 1991). However recent evidence suggests that hydraulic signal-induced ABA biosynthesis has to be decoded in the shoot, before leading to ABA action (Christmann et al., 2013; Endo et al., 2008). Christmann et al. (2007) showed that a root-evoked hydraulic signal resulted in local Ψ_l changes and, concomitantly, in turgor changes, which preceded ABA signaling and stomatal closure. Actually, ABA has been hypothesized to act downstream of the hydraulic signal in communicating water stress between roots and shoot (Christmann et al., 2007). Since water deficit reprensents a severe challenge for the maintenance of a proper plant water status, a combination of hydraulic and chemical signals might cooperate in mediating the root-to-shoot communications during drought stress (Davies & Zhang, 1991; Davies et al., 2005; Zhang et al., 2006).

Chemical signaling in response to drought stress involves the phytohormone ethylene in addition to ABA (Johnson & Ecker, 1998). The crosstalk between these two signaling pathways has been reported in response to a wide range of abiotic stresses (Beaudin et al., 2000). Ethylene is involved in root growth and stomatal opening, functions that are also under strong control by ABA (Wilkinson & Davies, 2010; Madhavan et al., 1983). In addition, ethylene may negatively regulate ABA signal generation (Ghassemian et al., 2000) as well as render stomatal less sensitive to ABA (Chen et al., 2013). By contrast, ABA restricts ethylene biosynthesis under water stress conditions (Sharp, 2002). Despite these advances in our understanding of the interaction between ethylene and ABA, the relationship between these two phytohormones in mediating the root-to-shoot signaling during drought stress remains a long-standing question, which has not been examined in depth.

In our study, we investigated the responses of *Populus nigra*, an isoprene emitting species, to different water regimes with the aim of dissecting hydraulic and chemical components of root-to-shoot signaling, investigating the potential link between isoprene and ABA biosynthesis, and estimating the interaction effects of ABA and ethylene. Plants were therefore grown in a split-root system in which both root halves were fully irrigated (well-watered plants, WW), a root half (WD) or both root halves (DD) suffered from water deprivation. In WD plants the hydraulic signal is indeed reduced thus allowing the estimation of hormone-mediated root-to-shoot

signaling. On the other hand, hormone and hydraulic root-to-shoot signaling operate concomitantly in DD plants in mediating plant response to water stress.

4.2 Materials and Methods

4.2.1 Plant material and split-root system

One year before the experiment, *Populus nigra* L. cuttings from a clonal provenance trial in Italy were planted in 6 dm^3 pots containing a 1:1:1 mixture of sand:peat:loam. Saplings grew outdoor under natural sunlight irradiance, and supplied (at two-week-interval) with Hoagland's solution. The following year, before budburst, the root apparatus of each sapling was vertically partitioned, and each root portion grew in 4 dm^3 pots (containing the same soil mixture used for saplings growth). The saplings grew in the split-root system over a two-month-period, and then exposed to different water treatments over a five-day-period: (1) optimal irrigation to both root compartments (WW); (2) withholding water to one compartment (WD) or (3) withholding water to both root compartments (DD).

4.2.2 Leaf gas exchange and chlorophyll fluorescence

Gas exchange and chlorophyll fluorescence measurements were performed on the central portion of newly expanded poplar leaves, using a portable infrared gas analyzer (IRGA) LI-6400 (Li-Cor, Inc., Nebraska, USA), mounting a 2 cm^2 leaf chamber equipped with a fluorometer. Operating conditions were the following: photosynthetic photon flux density (PPFD) of 1000 µmol m^{-2} s^{-1} (provided by red and blue light diode source), CO_2 concentration fixed of 390 ppm, relative humidity between 40 and 50%, leaf temperature of 30 °C. In detail, we determined net photosynthesis (A), stomatal conductance to water (g_s), intercellular CO_2 concentration (C_i) and electron transport rate (*ETR*). The *ETR* estimation was based on chlorophyll fluorescence measurement of the quantum yield of PSII in light adapted state (Φ_{PSII}), by multiplying Φ_{PSII} × incident PPFD × 0.5 (two photons are used to excite one electron), and × 0,87 (the leaf absorbance coefficient), as indicated by Krall & Edwards (1992).

4.2.3 Isoprene emission

After gas exchange measurements the outlet gas flow from the IRGA chamber was conveyed through a polytetrafluoroethylene (PTFE) tube to a proton transfer reaction time-of-

flight mass spectrometer (PTR-TOF 2000; Ionicon, Innsbruck, Austria) to measure, on-line, the isoprene emission from the leaf. The foliar emission of isoprene was calculated by subtracting background measurements of gas from the empty cuvette, and normalizing the datum to both flow rate inside the chamber and leaf portion dry weight.

4.2.4 Water status

Plant water status was estimated through measurements of leaf water potentials (Ψ_l), which were performed after gas exchange measurements on fully expanded leaves using a standard methodology, through a Scholander-type pressure chamber (SKPM1400, Skye Instruments, Llandrindod Wells, UK).

4.2.5 Analysis of free-ABA and ABA-GE

Fresh leaf tissue (300-350 mg) was added with 50 ng of D6-ABA, 50 ng of d5-ABA-GE and then extracted with 3 mL of CH_3OH/H_2O (pH 2.5 with HCOOH) at 4°C for 30 minutes. The supernatant was partitioned 3 times with 3 mL of n-exane. The aqueous-methanolic phase was collected and then purified with Sep-Pak C18 cartridges (Waters, Massachusetts, USA). The sample solutions were loaded onto the Sep-Pak C18 cartridges and washed with 2 mL of water pH 2.5. ABA and ABA-GE were eluted by 1.2 mL of ethylacetate. The eluate was dried under nitrogen and rinsed with 500 µL CH_3OH/H_2O pH 2.5. Identification and quantification of free-ABA and ABA-GE was performed injecting 3 µL in LC-ESI-MS/MS, using an Agilent LC1200 chromatograph coupled with an Agilent 6410 triple quadrupole MS detector equipped with an ESI source (all from Agilent Technologies, Santa Clara, CA, USA). Analyses were performed in negative ion mode. Compounds were separated in a Poroshell C_{18} column (3.0 x 100 mm, 2.7 µm i.d., Agilent, USA) using a binary solvent system comprising water with 0.1 % of HCOOH (solvent A) and acetonitrile/methanol (1/1) (added with 0.1 % of HCOOH, solvent B). The solvent gradient was programmed to change linearly from 95% A to 100% B during a 30-min run at a flow-rate of 0.3 $mLmin^{-1}$. Quantification was conducted in multiple reaction mode (MRM) as reported in López-Carbonell 2009.

4.2.6 Ethylene emission

Ethylene emission rate was measured on leaves (300 to 500 mg fresh weight) detached from each sapling, enclosed in 50 ml glass vials with airtight seal, and incubated at PPFD of

1000 µmol m^{-2} s^{-1} for over a 60-min-period. Ethylene concentration was measured extracting the headspace from the vial, flushing air through the seal at a flow-rate of 200 mL s^{-1} and directing the gas to the PTR-TOF using a short PTFE tube. The detection of ethylene using the PTR-TOF has been possible using O_2^+ as ionizing agent (Biasioli et al, 2010). The ethylene emission rate was determined by subtracting background measurements and normalizing the ethylene concentration in the sample headspace to both sample dry weight, vial volume and incubation time.

4.2.7 ACC analysis

The concentration of ACC (1-aminocyclopropane-1-carboxylic acid) was determined according to the protocols previously reported by Concepcion et al. 1979 and by Bulens et al. 2011. This is a sensitive method for the quantitative determination of ACC base on the oxidation of ACC to ethylene. Fresh leaf tissue (300-350 mg) was extracted with 1 mL of a aqueous solution of sulfosalicylic acid (5%) for 30 minutes at 4°C. Extracts were centrifuged at 4°C for 10 min (3000 x g) , 600 µL of the supernatant collected in a 20 mL glass GC-vial and 200 µL of a 10 mM $HgCl_2$ aqueous solution added. The reaction vials were capped with rubber serum stoppers and aluminum caps, then added with 200 µL of a NaOH/NaOCl (2/1) mixture. Reaction mixtures were shaken for 5 minutes and maintained for 4 minutes on ice, after which ethylene was measured using an ethylene detector ETD-300 with valve control box (all from Sensor Sense B.V., Nijmegen, The Netherlands). The gas flow was 3 L/h. The acquisition time was of 8 minutes for the sample and 2 minutes for the blank. The quantification was performed using a six-points calibration curve of authentic ACC standard (Sigma Aldrich, Milan, Italy).

4.2.8 Statistics

Four replicates for each water treatment were measured during the experiment. Data were first tested by a repeated-measures analysis with ANOVA, to evaluate the effects of both time and treatment on the measured parameters. In the single dates, differences within treatments were tested by a one-way ANOVA analysis and means were compared using the Student-Newman-Keuls post hoc test, with a significance level $P = 0.05$. All analyses were conducted using IBM SPSS 20.0 software (SPSS Inc., Chicago, USA).

4.3 Results

4.3.1 Gas exchange, PSII performance and leaf water potential are affected only in DD leaves

Plants in which both root portions suffered from water deprivation (DD) showed significant declines in gas exchange performance. Declines in A, and particularly in g_s were early effects of drought stress, as differences with respect to WW plants were significant just after two days of treatment (Fig. 4.1 a,b). Reductions in A and g_s became much more evident as drought stress progressed such that in DD leaves net photosynthesis and stomatal conductance accounted for 10% and 4% of corresponding values in WW leaves. Limitation to photosynthesis were mostly stomatal, as C_i rapidly declined following g_s decreases during the first three days of drought stress and then remained about 40% lower than gs in WW and WD plants (Fig. 4.1 c,b). Leaf functioning of plants in which only one portion of the root system suffered from drought (WD) did not differ from that of WW plants. Net assimilation rate (A) (Fig. 4.1 a) and stomatal conductance (g_s) (Fig. 4.1 b) increased in both WW and WD during the experimental period. It is possible that changes in external conditions have been responsible for this unexpected behavior, which, however, did not regard DD leaves.

Data of gas exchange are consistent with plant water status. Indeed, Ψ_l declined early in response to drought in DD leaves, whereas it was unaffected in WD leaves. Leaf water potential did not decline significantly in DD leaves from day 2 (-0.98 MPa) to day 5 (-1.25 MPa) (Fig. 4.2 and Table 4.1), conforming to the rapid decrease in g_s observed over the same experimental period. The stress-induced limitation of photosynthesis determined a progressive increase of the ratio between the electron transport rate and net CO_2 assimilation (ETR / A) in DD plants, that reached a value of ~47 at day 5 (Fig 4.1 d), which was about five times higher than ETR/A in WW and WD plants.

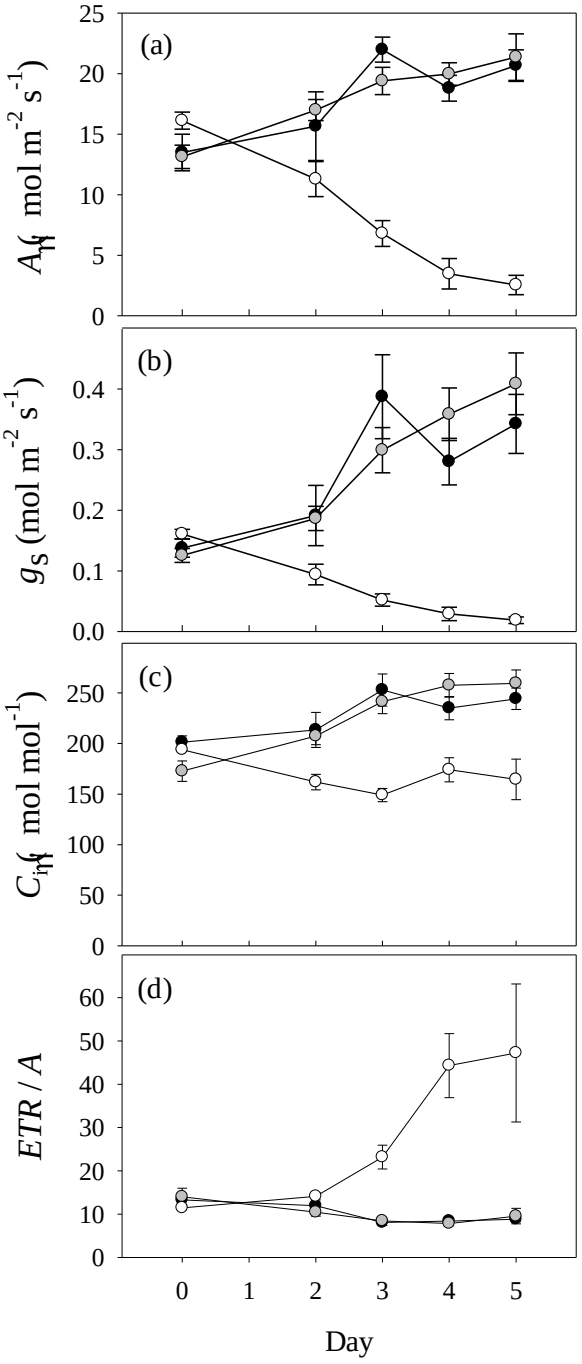

Fig. 4.1: Leaf net photosynthesis (A), stomatal conductance (g_s), intercellular CO_2 concentration (C_i) and electron transport rate / photosynthesis ratio (ETR / A) measured on *Populus nigra* saplings subjected for five days to different water treatments: full irrigation of the root system (WW, black symbols), partial root zone drying (WD, gray symbols) and complete drying (DD, white symbols). Data represent means of each treatment ± SE.

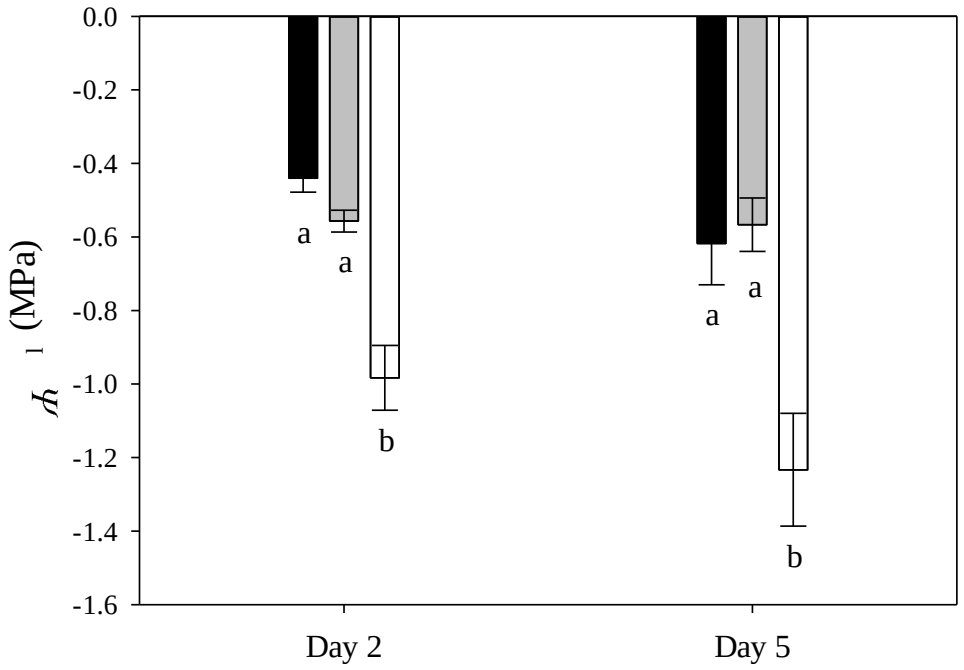

Fig. 4.2: Leaf water potentials in *Populus nigra* saplings measured on the second and the fifth day of three different water treatments: full irrigation of the root system (WW, black bars), partial root zone drying (WD, gray bars) and complete drying (DD, white bars). Data represent means of each treatment ± SE. Different letters indicate significant difference between treatments in the same day ($P < 0.05$).

Table 1. Repeated measures analysis of variance for leaf water potential (Ψ_l), Isoprene emission, ABA and ABA-GE concentration in *Populus nigra* saplings measured on the second and the fifth day of three different water treatments. Significance values are indicated as *** = $P<0.001$, ** = $P<0.01$, * = $P<0.05$.

Source	F statistic		
	Time	Treatment	Time x Treatment
Ψ_l	4.1^{ns}	23.7^{**}	1.1^{ns}
Isoprene	0.0^{ns}	12.9^{**}	0.2^{ns}
ABA	66.6^{***}	100.9^{***}	70.1^{***}
ABA-GE	5.0^{ns}	7.1^{*}	31.6^{**}

4.3.2 Isoprene emission is decoupled from photosynthesis

Isoprene emission was higher (on average +50%) in DD leaves than in both WW and WD leaves throughout the experiment, indicating that isoprene biosynthesis did not relate with photosynthesis. Isoprene emission did not indeed decrease as drought stress progressed in DD leaves, though photosynthesis declined as much as 80% from day 2 to day 5. We calculate that

percent of photosynthetic carbon lost as isoprene was 0.7, 0.86 and 1.77 in WW, WD, and DD leaves respectively, after two days of irrigation treatment. Carbon lost to isoprene biosynthesis was ~ 0.60% both in WW and WD leaves at the end of the experiment, whereas the percent of fresh assimilated carbon emitted as isoprene increased up to 7.4% in DD leaves.

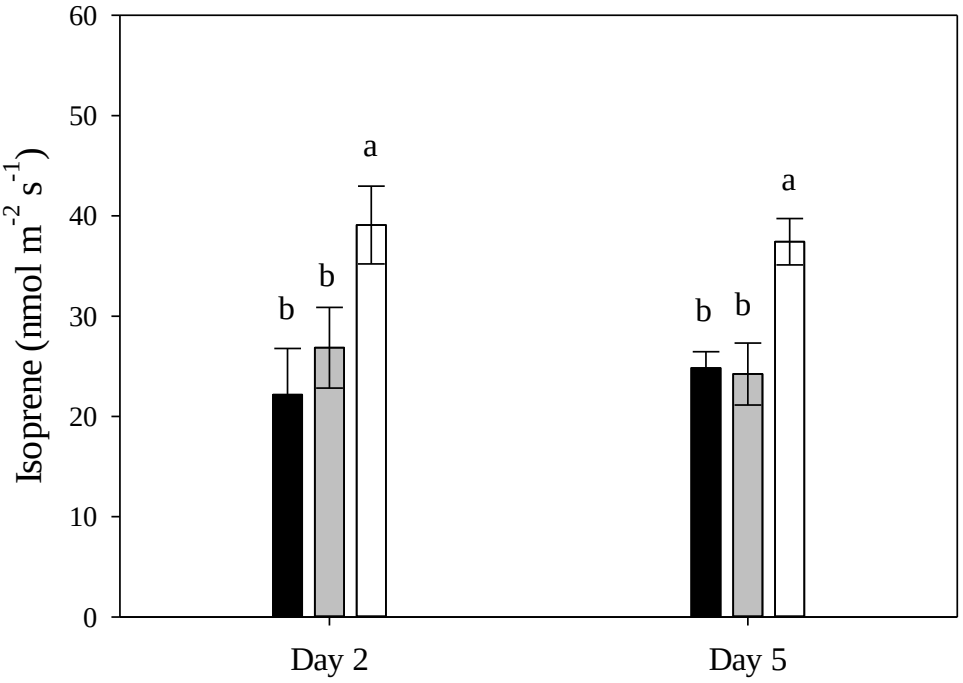

Fig. 4.3: Isoprene emission rate in *Populus nigra* leaves measured on the second and the fifth day of three different water treatments: full irrigation of the root system (WW, black bars), partial root zone drying (WD, gray bars) and complete drying (DD, white bars). Data represent means of each treatment ± SE. Different letters indicate significant difference between treatments in the same day ($P < 0.05$).

4.3.3 Free-ABA and ABA-GE concentrations are higher in DD than in WW and WD leaves

Overall, leaf ABA concentration (pooling together free-ABA and ABA-GE) was on average 91% greater in DD than in WW and WD plants. An increase in the concentration of free-ABA was an early effect of DD treatment, whereas both free-ABA and ABA-GE increased in concentration from day 2 to day 5. The accumulation of active and inactive pools of ABA in DD leaves was unrelated with leaf water potential, which varied little as drought stress progressed. The ratio of free-ABA to ABA-GE also markedly differ in differentially irrigated leaves, ranging from 0.05 in WW to 0.07 in WD up to 0.44 in DD leaves.

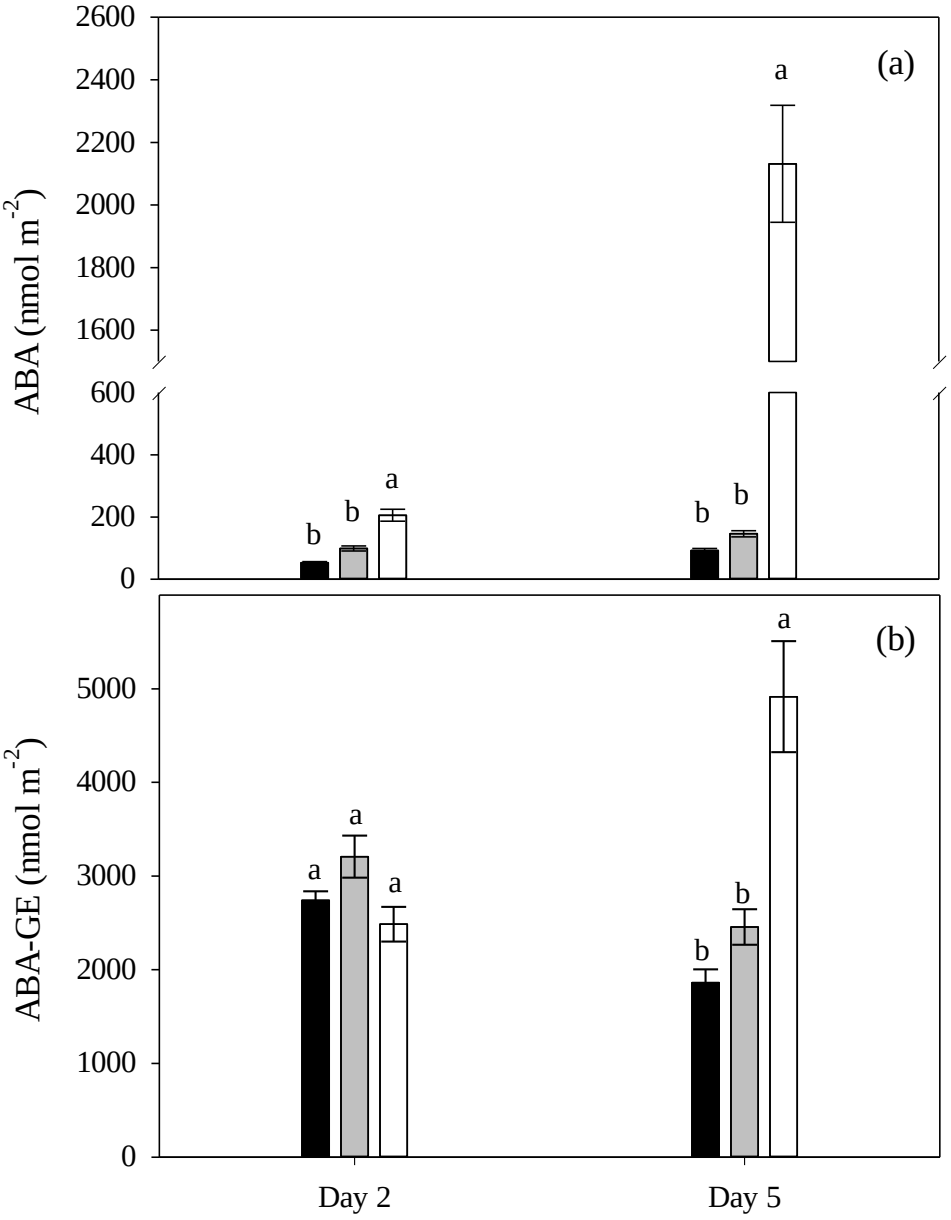

Fig. 4.4: Free ABA and ABA-GE concentrations in *Populus nigra* laves measured on the second and the fifth day of three different water treatments: full irrigation of the root system (WW, black bars), partial root zone drying (WD, gray bars) and complete drying (DD, white bars). Data represent means of each treatments ± SE. Different letters indicate significant difference between means in the same day ($P < 0.05$).

4.3.4 Ethylene emission is higher in WD than in WW and DD leaves

The emission of ethylene and the concentration of its precursor ACC, measured at the end of the experiment, were markedly affected by irrigation treatments. Ethylene evolution was indeed 75% or 100% higher in WD than in WW or DD leaves, respectively. On the contrary,

ACC levels were much higher (on average +95%) in DD leaves than in corresponding WW and WD ones.

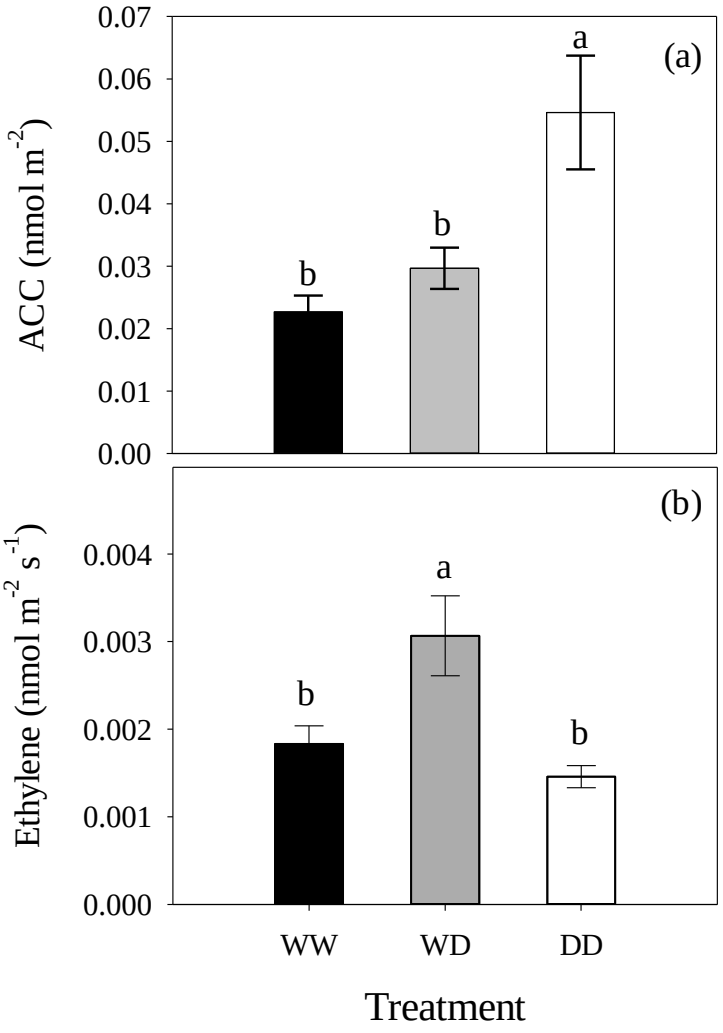

Fig. 4.5: ACC concentration and ethylene emission rate in *Populus nigra* laves measured on the second and the fifth day of different water treatments: full irrigation of the root system (WW, black bars), partial root zone drying (WD, gray bars) and complete drying (DD, white bars). Data represent means of each treatments ± SE. Different letters indicate significant difference between means ($P < 0.05$).

4.4 Discussion

Plants in which both root portions were deprived of water (DD) underwent steep drop in Ψ_l early during stress imposition. This response was not accompanied by similar decreases in stomatal conductance, indicating a classical anisohydric behavior in poplar, and allowed to maintain appreciable net photosynthesis. This suggests that in DD plants the hydraulic component of stomatal regulation may prevail over the chemical one (Damour et al., 2010; McAdam &

Brodribb, 2013; Schachtman & Goodger, 2008) during early stage of stress imposition. This is also consistent with the lack of variations in Ψ_l and gas exchange performance in WD plants, in which the hydraulic signal is actually reduced. Indeed, even thought spilt root plants received half the water applied to WW plants, water uptake from roots was sufficient to equilibrate plant water potential and maintain Ψ_l (Sobeih et al., 2004). However, as drought stress progressed poplar leaves underwent previously reported switch from anisohydric to isohydric behavior (Domec & Johnson, 2012), in which a tight control of stomatal opening operates, thus maintaining leaf hydration, as revealed by little variation in Ψ_l from day 2 to day 5 in DD leaves.

Overall, our study suggests that hydraulic signal is likely upstream of the chemical signal driven by ABA biosynthesis and accumulation (Christmann et al., 2013). Indeed in DD leaves hydraulic signal triggered an early slight accumulation of foliar free-ABA (from 52.1 nmol m^{-2} s^{-1} in WW to 205.8 nmol m^{-2} s^{-1} in DD, Fig. 4a), whereas a dramatic increase in the concentration of free ABA (2131.5 nmol m^{-2} s^{-1}) was observed only at the end of drought stress imposition. This hydraulic-induced chemical signal was also likely responsible for the switch from anisohydric to isohydric behavior (Domec et al., 2012). Our hypothesis is further supported by observing that in WD plants changes in the concentrations of both free-ABA and ABA-GE were not detected with respect to WW plants. The increase in the concentrations of free-ABA and ABA-GE in DD leaves suggests that a relevant portion of foliar ABA is likely imported from the roots, and this root-derived signal could have been triggered by the hydraulic signal (Schachtman & Goodger, 2008). Nonetheless, the steep reduction in the ratio of inactive ABA (ABA-GE) to active ABA (free-ABA) in DD leaves as compared with WW and WD leaves, suggest that free ABA was also possibly generated from de-glucosylation of ABA-GE in the leaf. This low-cost pathway of free-ABA production permits plants to adjust ABA levels to meet physiological needs, i.e for a rapid control of stomatal opening, without diverting carbon for the biosynthesis of "essential" MEP-derived metabolites. In addition, this one-step process may provide severely stressed plants with an ABA-pool rapidly usable, to counter further stressful agents of unpredictable origin (Lee et al., 2006).

An increase in isoprene biosynthesis is an early response to drought stress (Beckett et al., 2012). Isoprene may indeed serve as a short-term thermo-protective agent under drought stress, e.g. in *Quercus* spp. (Brüggemann & Schnitzler, 2002). Isoprene production is usually related to photosynthesis, which provides nearly 70-90% of carbon for isoprene biosynthesis. Nonetheless, production of isoprene still occurs when photosynthesis is greatly inhibited under severe drought (Brilli et al., 2007), as we also observed in our experiment (Figs. 1 and 3). The great investment of carbon to isoprene biosynthesis during severe drought stress, as we observed in DD leaves after five days of withholding water, suggests a derived benefit from increased isoprene

production in poplar. It has been indeed suggested that isoprene production increases following a reduction in C_i due to stomatal closure, thereby maintaining electron transport when photosynthetic carbon fixation is reduced (Harrison et al., 2013). According to this hypothesis, drought induces an excess of reducing power, determined by a strong disproportion between electron transport rate and photosynthetic capacity (Fig. 1d); this leads to a consequent overproduction of ATP and NADPH that are channeled to DMADP and then to the synthesis of isoprene and other MEP-derived products. Actually, isoprene biosynthesis prevents the accumulation of DMADP, and hence channels more carbon to the biosynthesis of more complex MEP-derived products, including ABA (Rasulov et al., 2013). This was hypothesized to occur in transgenic tobacco plants transformed to emit isoprene, in which the concentration of foliar ABA was steeply higher than in leaves of non-emitting plants under severe drought (Tattini et al., 2014).

Our data do not evidence a clear relation between isoprene and ABA biosynthesis, likely because plant water status co-varied with isoprene emission, thereby making hard dissecting the hydraulic-driven from the isoprene-driven increase in foliar ABA concentration. Actually, our study suggests that hydraulic signal mostly regulated the accumulation of free-ABA and ABA-GE in poplar, as dramatic increases in both ABA forms in the leaf occurred during drought stress progression, without concomitant increases in isoprene emission. Nonetheless, we cannot exclude that isoprene biosynthesis may have contributed to enhance both *de-novo* free-ABA biosynthesis through the MEP pathway and hydrolysis of ABA-GE to form free-ABA in the leaf. An increase in isoprene biosynthesis coupled with reductions in photosynthetic carbon fixation rates may indeed render plants in a state of hyper-responsiveness to drought stress (Tattini et al., 2014), thus allowing a prompt re-distribution between inactive and active pool of ABA. This may have been of particular significance during mild soil water deficits when hydraulic signal is not indeed sufficient to promote massive root-to-shoot ABA movement. Actually, the ratio of ABA to ABA-GE was markedly higher in DD leaves (0.095) than in WW (0.022) and WD leaves (0.035) early during stress imposition. Our hypothesis conforms to previous suggestions that isoprene biosynthesis may indeed correlate to a labile and active pool of foliar ABA, which is responsible for stomata regulation (Barta & Loreto, 2006). Our data suggest that the first long-distance signal is a root-derived hydraulic signal, which results in a decreased leaf Ψ_l in DD plants. The perception of the changes in Ψ_l leads to the conversion of the hydraulic signal into the chemical ABA signal. In addition, the increasing ABA-GE content in DD poplars enables plants to accomplish a rapid increment in free-ABA levels, intensifying an effective stress signal in response to dehydration (Lee et al., 2006).

Our study reveals a clear antagonism between ABA and ethylene emission by the leaf during drought stress in poplar (Raghavendra et al., 2010; Goodger, 2013; Morgan et al., 1997). Ethylene is indeed produced in the leaf following the root to shoot transport of its precursor ACC (Else and Jackson, 1998) during drought stress. The increase in ethylene production may counter ABA-induced stomatal closure (Tanaka et al., 2005), possibly enhancing ABA catabolism (Spollen et al., 2000). These suggestions fit well with our observation in WD plants, in which the emission of ethylene largely exceeds those in WW and DD leaves (Sobeih et al., 2004). Indeed the concentration of ACC did not markedly differ between WW and WD leaves, whereas ethylene emission was ~70% higher in the latter than in the former leaves. On the other hand, ACC accumulated to a great extent in DD leaves (+75% as compared with WD leaves) and the emission rate of ethylene was much lower than that in WD leaves. We interpret these results on the basis of the strength of hydraulic signals generated in plants having one or both root portions suffering from water withholding. The strong hydraulic signal originated in DD plants mostly promoted the biosynthesis of ABA that moved from root to shoot. Then, the high foliar ABA concentration inhibited the conversion of ACC to produce ethylene (Chen et al., 2013; Sharp et al. 2002). In contrast, in the absence of relevant hydraulic signal as likely occurred in WD plants, root-derived ethylene may have inhibited accumulation of foliar ABA as well as its control on stomatal opening.

References

Affek, H. P., Yakir, D., 2003. Natural abundance carbon isotope composition of isoprene reflects incomplete coupling between isoprene synthesis and photosynthetic carbon flow. Plant Physiology, 131(4), 1727-1736.

Barta, C., Loreto, F., 2006. The relationship between the methyl-erythritol phosphate pathway leading to emission of volatile isoprenoids and abscisic acid content in leaves. Plant physiology, 141(4), 1676-1683.

Beckett M., Loreto F., Velikova V., Brunetti C., Di Ferdinando M., Tattini M., Calfapietra C., Farrant J.M. 2012. Photosynthetic limitations and volatile and non-volatile isoprenoids in the poikilochlophyllus resurrection plant *Xerophyta humilis* during dehydration and rehydration. Plant, Cell & Environent 35, 2061-2074.

Beaudoin N., Serizet C., Gosti F., Giraudat J. 2000. Interactions between abscisic acid and ethylene signaling cascades. The Plant Cell. 12 (7), 1103-1115.

Brilli F., Barta C., Fortunati A., Lerdau M., Loreto F., Centritto M., 2007. Response of isoprene emission and carbon metabolism to drought in white poplar (*Populus alba*) saplings. New Phytologist 175, 244-254

Mc Adam S.A.M. and Brodribb T.J. 2013. Ancestral stomatal control results in a canalization of fern and lycophyte adaptation to drought. New Phytologist, 198, 429-441.

Biasioli, F., Gasperi, F., Yeretzian, C., Märk, T. D., 2011. PTR-MS monitoring of VOCs and BVOCs in food science and technology. Trends in Analytical Chemistry, *30*(7), 968-977.

Brüggemann, N., Schnitzler, J. P., 2002. Comparison of Isoprene Emission, Intercellular Isoprene Concentration and Photosynthetic Performance in Water-Limited Oak (*Quercus pubescens* Willd. and *Quercus robur* L.) Saplings. Plant Biology, 4(4), 456-463.

Bulens I., Van de Poel B., Hertog M.L., De Proft M.P., Geeraerd A.H., Nicoläi B.M. 2011. Protocol: an updated integrated methodology for analysis of metabolites and enzyme activities of ethylene biosynthesis. Plant Methods 7: 17.

Centritto, M., Brilli, F., Fodale, R., Loreto, F., 2011. Different sensitivity of isoprene emission, respiration and photosynthesis to high growth temperature coupled with drought stress in black poplar (*Populus nigra*) saplings. Tree physiology, 31(3), 275-286.

Chen, L., Dodd, I. C., Davies, W. J., Wilkinson, S., 2013. Ethylene limits abscisic acid-or soil drying-induced stomatal closure in aged wheat leaves. Plant, cell & environment, 36(10), 1850-1859.

Christmann A., Erwin G., Huang J. 2013. Hydraulic signals in long-distance signaling. Current Opinion in Plant Biology, 16, 293-300.

Christmann A., Weiler E.W., Steudle e., Grill E. 2007. A hydraulic signal in root-to-shoot signalling of water shortage. The Plant Journal, 52, 167-174.

Concepcion M., Lizada C, Yang S.F. 1979. A simple and sensitive assay for 1-aminocyclopropane-1-carboxylic acid. Analytical biochemistry, 100, 140-145.

Damour G., Simonneau T., Cochard H., Urban L. 2010. An overview of models of stomatal conductance at the leaf level. Plant, Cell and Environment, 33, 1419-1438.

Davies, W. J., Zhang, J., 1991. Root signals and the regulation of growth and development of plants in drying soil. Annual review of plant biology, 42(1), 55-76.

Davies, W.J., Kudoyarova G., Hartung W. 2005. Long-distance ABA signalling and its relation to other signalling pathways in the detection of soil drying and the mediation of the plant's response to drought. Journal of Plant Growth and Regulation 24, 285-295.

Desikan, R., Cheung, M. K., Bright, J., Henson, D., Hancock, J. T., Neill, S. J. 2004. ABA, hydrogen peroxide and nitric oxide signalling in stomatal guard cells. Journal of experimental botany, 55(395), 205-212.

Domec, J. C., Johnson, D. M., 2012. Does homeostasis or disturbance of homeostasis in minimum leaf water potential explain the isohydric versus anisohydric behavior of *Vitis vinifera* L. cultivars?. Tree physiology, 32(3), 245-248.

Else, M. A., and Jackson, M. B., 1998. Transport of 1-aminocyclopropane-1-carboxylic acid (ACC) in the transpiration stream of tomato (*Lycopersicon esculentum*) in relation to foliar ethylene production and petiole epinasty. Functional Plant Biology, 25(4), 453-458.

Endo A., Sawada Y., Takahashi H., Okamoto M., Ikegami K., Koiwai H., Seo M., Toyomasu T., Mitsuhashi W., Shinozaki K., et al. Drought induction of Arabidopsis 9-cis-epoxycarotenoid dioxygenase occurs in vascular parenchyma cells. Plant Physiology, 2008, 1984-1993.

Fall, R., Monson, R. K., 1992. Isoprene emission rate and intercellular isoprene concentration as influenced by stomatal distribution and conductance. Plant physiology, 100(2), 987-992.

Funk, J. L., Mak, J. E., Lerdau, M. T., 2004. Stress-induced changes in carbon sources for isoprene production in Populus deltoides. Plant, Cell & Environment, 27(6), 747-755.

Ghassemian M., Nambara E., Cutler S., Kawaide H., Kamiya Y., McCourt P. 2000. Regulation of abscisic acid signaling by the ethylene response pathway in Arabidopsis. Plant Cell 12, 1117-1126.

Goodger, J. Q., 2013. Long-Distance Signals Produced by Water-Stressed Roots. In: Long-Distance Systemic Signaling and Communication in Plants (pp. 105-124). Springer Berlin Heidelberg.

Guidolotti, G., Calfapietra, C., Loreto, F., 2011. The relationship between isoprene emission, CO_2 assimilation and water use efficiency across a range of poplar genotypes. Physiologia plantarum, 142(3), 297-304.

Harrison, S. P., Morfopoulos, C., Dani, K. G., Prentice, I. C., Arneth, A., Atwell, B. J., Barkley, M. P., Leishman, M. R., Loreto, F., Medlyn, B. E., Niinemets, Ü., Possell, M.,Peñuelas, J., Wright, I. J., Wright, I. J., 2013. Volatile isoprenoid emissions from plastid to planet. New Phytologist, 197(1), 49-57.

Johnson P.R. and Ecker J.R. 1998. The ethylene gas signal transduction pathway: a molecular perspective. Annual Review of Genetics. 32, 227-254.

Karl, T., Fall, R., Rosenstiel, T., Prazeller, P., Larsen, B., Seufert, G., Lindinger, W., 2002. On-line analysis of the $^{13}CO_2$ labeling of leaf isoprene suggests multiple subcellular origins of isoprene precursors. Planta, 215(6), 894-905.

Krall, J. P., Edwards, G. E., 1992. Relationship between photosystem II activity and CO2 fixation in leaves. Physiologia Plantarum, 86(1), 180-187.

Kreuzwieser J., Graus M., Wisthaler A., Hansel A., Rennenberg H., Schnitzler J-P. 2002. Xylem-transported glucose as an additional carbon source for leaf isoprene formation in *Quercus robur*. New Phytologist, 156: 171-178.

Lee, K. H., Piao, H. L., Kim, H. Y., Choi, S. M., Jiang, F., Hartung, W., Hwang, I., Kwak, J. M., Lee, I. J., Hwang, I., 2006. Activation of glucosidase via stress-induced polymerization rapidly increases active pools of abscisic acid. Cell, 126(6), 1109-1120.

Lichtenthaler H. K., Rohmer M., Schwender J., 1997. Two independent biochemical pathways for isopentenyl diphosphate and isoprenoid biosynthesis in higher plants. Physiologia Plantarum, 101, 643-652.

Liu, F., Andersen, M. N., Jacobsen, S. E., Jensen, C. R. 2005a. Stomatal control and water use efficiency of soybean (*Glycine max* L. Merr.) during progressive soil drying. Environmental and Experimental Botany, 54(1), 33-40.

Liu, F., Jensen, C. R., Shahanzari, A., Andersen, M. N., Jacobsen, S. E., 2005b. ABA regulated stomatal control and photosynthetic water use efficiency of potato *Solanum tuberosum* L.) during progressive soil drying. Plant Science, 168(3), 831-836.

López-Carbonell M., Gabasa M., Jáuregui O. 2009. Enhanced determination of abscisic acid (ABA) and abscisic acid glucose ester (ABA-GE) in Cistus albidus plants by liquid

chromatography-mass spectrometry in tandem mode. Plant Physiology and Biochemistry, 47, 256-261.

Loreto, F., Velikova, V., 2001. Isoprene produced by leaves protects the photosynthetic apparatus against ozone damage, quenches ozone products, and reduces lipid peroxidation of cellular membranes. Plant Physiology, *127*(4), 1781-1787.

Madhavan S., Chrominiski A., Smith B.N. 1983. Effect of ethylene on stomatal opening in tomato and carnation leaves. Plant Cell Physiol, 24 (3), 569-572.

Morgan, P. W. Drew, M. C.,1997. Ethylene and plant responses to stress. Physiol. Plant. 100:620-530.

Pantin, F., Monnet, F., Jannaud, D., Costa, J. M., Renaud, J., Muller, B., Simonneau, T., Genty, B., 2013. The dual effect of abscisic acid on stomata. New Phytologist, 197(1), 65-72.

Peñuelas J. and Llusià J. 2003. BVOCs: plant defense against climatic warming? Trends in Plant Science, 8: 105-109.

Pegoraro, E., Rey, A., Greenberg, J., Harley, P., Grace, J., Malhi, Y., Guenther, A., 2004. Effect of drought on isoprene emission rates from leaves of *Quercus virginiana* Mill. Atmospheric Environment, 38(36), 6149-6156.

Raghavendra A.S., Gonugunta V.K., Christmann A., Grill E. 2010. ABA perception and signalling. Trends in Plant Science. 15, 395-401.

Rasulov B., Bichele I., Laisk A., Niinemets Ű. 2013. Competition between isoprene emission and pigment synthesis during leaf development in aspen. Plant, Cell and Environment,

Schachtman D.P. and Goodger J.Q.D. 2008. Chemical root to shoot signaling under drought. Trends in Plant Science. 13, 281-287.

Schnitzler, J. P., Louis, S., Behnke, K., Loivamäki, M., 2010. Poplar volatiles–biosynthesis, regulation and (eco) physiology of isoprene and stress-induced isoprenoids. Plant Biology, 12(2), 302-316.

Sharkey, T. D., Loreto, F., 1993. Water stress, temperature, and light effects on the capacity for isoprene emission and photosynthesis of kudzu leaves. Oecologia, 95(3), 328-333.

Sharp, R. E., 2002. Interaction with ethylene: changing views on the role of abscisic acid in root and shoot growth responses to water stress. Plant, Cell & Environment, *25*(2), 211-222.

Sobeih, W. Y., Dodd, I. C., Bacon, M. A., Grierson, D., Davies, W. J., 2004. Long-distance signals regulating stomatal conductance and leaf growth in tomato (Lycopersicon esculentum) plants subjected to partial root-zone drying. Journal of Experimental Botany, 55(407), 2353-2363.

Spollen, W. G., LeNoble, M. E., Samuels, T. D., Bernstein, N., Sharp, R. E. (2000). Abscisic acid accumulation maintains maize primary root elongation at low water potentials by restricting ethylene production. Plant Physiology, 122(3), 967-976.

Tanaka, Y., Sano, T., Tamaoki, M., Nakajima, N., Kondo, N., Hasezawa, S., 2005. Ethylene inhibits abscisic acid-induced stomatal closure in Arabidopsis. Plant Physiology, 138(4), 2337-2343.

Tattini M., Montagni G., Traversi M.L. 2002. Gas exchange, water relations and osmotic adjustment in Phyllirea latifolia grown at various salinity concentrations. Tree Physiology, 22, 403-412.

Tattini et al. 2014. Isoprene protects transgenic tobacco plants from severe drought stress through alteration of isoprenoids, non-structural carbohydrates and phenylpropanoids metabolism. Plant Cell Environ.

Velikova, V., Várkonyi, Z., Szabó, M., Maslenkova, L., Nogues, I., Kovács, L., Peeva, V., Busheva, M., Garab, G., Sharkey, T, D., Loreto, F., 2011. Increased thermostability of thylakoid membranes in isoprene-emitting leaves probed with three biophysical techniques. Plant Physiology, 157(2), 905-916.

Vickers, C. E., Gershenzon, J., Lerdau, M. T., Loreto, F., 2009a. A unified mechanism of action for volatile isoprenoids in plant abiotic stress. Nature Chemical Biology, 5(5), 283-291.

Wilkinson, S., Davies, W. J., 2010. Drought, ozone, ABA and ethylene: new insights from cell to plant to community. Plant, cell & environment, 33(4), 510-525.

Wolfertz, M., Sharkey, T. D., Boland, W., Kühnemann, F., 2004. Rapid regulation of the methylerythritol 4-phosphate pathway during isoprene synthesis. Plant physiology, 135(4), 1939-1945.

Zhang J., Jia W., Yang J., Ismail A.M. 2006. Role of ABA in integrating plant responses to drought and salt stresses. Field Crop Research, 97, 111-119.